Towards the Stable Chelation of Radium for Biomedical Applications with an 18-Membered Macrocyclic Ligand

Diane S. Abou,‡[a,b,c] Nikki A. Thiele,‡[d,e] Nick T. Gutsche,[f] Alexandria Villmer,[a,b] Hanwen Zhang,[a,b] Joshua J. Woods,[d,g] Kwamena E. Baidoo,[f] Freddy E. Escorcia,[f] Justin J. Wilson*[d] and Daniel L. J. Thorek*[a,b,h,i]

(‡) These authors contributed equally to this work.

Affiliations:
[a]Department of Radiology, Washington University in St. Louis School of Medicine, St. Louis, MO 63110, USA. E-mail: thorek.lab@wustl.edu
[b]Program in Quantitative Molecular Therapeutics, Washington University in St. Louis School of Medicine, St. Louis, MO 63110, USA
[c]Radiology Cyclotron Facility, Mallinckrodt Institute of Radiology, Washington University in St. Louis, St. Louis, MO 63110, USA
[d]Department of Chemistry and Chemical Biology, Cornell University, Ithaca, NY 14853, USA. E-mail: jjw275@cornell.edu.
[e]Chemical Sciences Division, Oak Ridge National Laboratory, Oak Ridge, TN 37830, USA
[f]Molecular Imaging Program, Center for Cancer Research, National Cancer Institute, National Institutes of Health, Bethesda, MD 20892, USA
[g]Robert F. Smith School for Chemical and Biomolecular Engineering, Cornell University, Ithaca, NY 14853 USA
[h]Department of Biomedical Engineering, Washington University in St. Louis, St. Louis, MO 63110, USA
[i]Oncologic Imaging Program, Siteman Cancer Center, Washington University in St. Louis School of Medicine, St. Louis, MO 63110, USA

* Co-corresponding authors to whom correspondence should be addressed.

Daniel Thorek, PhD.
Molecular Radiotherapy and Imaging Laboratory
Program in Quantitative Molecular Therapeutics
Mallinckrodt Institute of Radiology
Washington University School of Medicine
510 S. Kingshighway Blvd. Campus Box 8225
St. Louis, Missouri, 63108
thorek.lab@wustl.edu

Justin Wilson, PhD.
Department of Chemistry and Chemical Biology
Baker Laboratory
Cornell University
Chemistry Research Building
162 Sciences Drive, Ithaca, NY 14853
jjw275@cornell.edu

TABLE OF CONTENTS

page

LIST OF TABLES

Table page

LIST OF FIGURES

Figure page

1. EXPERIMENTAL PROCEDURES

1.1 DFT calculations for Ba^{2+} and Ra^{2+} complexes of macropa

Density functional theory (DFT) calculations were carried out to model the expected geometry of [Ra(macropa)] in comparison to [Ba(macropa)]. Calculations were performed using *Gaussian09* software.[1] The structures of [Ba(macropa)(OH_2)] and [Ra(macropa)(OH_2)] were optimized at the TPSSh level of theory.[2,3] Light atoms (H, O, N, C) were treated with the triple zeta valence potential (TZVP) basis set of Ahlrichs and coworkers,[4,5] and the metal atoms were handled using their respective large core relativistic effective core potential with the associated basis sets (ECP46MDF for Ba and ECP78MDF for Ra).[6] The crystal structure of the Ba^{2+} complex of macropa shows the presence of a coordinated water molecule penetrating the macrocyclic core.[7] As such, geometry optimizations of the Ba^{2+} and Ra^{2+} complexes of macropa were run starting with one inner-sphere water molecule and two outer-sphere water molecules. The two outer-sphere water molecules were added to the optimization because in their absence the position of the lone coordinated water molecule moved to the outer sphere to hydrogen bond with the ligand. The additional outer-sphere water molecules provide hydrogen-bonding partners for this donor and better simulate the expected environment in aqueous solution. Figure S1 shows an overlay of the calculated geometries for both complexes. The calculated interatomic distances for the two complexes are presented in Table S1. Optimized coordinates are provided in Tables S2 and S3. The interatomic distances for [Ra(macropa)(OH_2)]·$2H_2O$ are slightly albeit systematically larger than those for [Ba(macropa)(OH_2)]·$2H_2O$ due to the larger ionic radius of Ra^{2+} compared to Ba^{2+}. Examination of the optimized structures of the two complexes shows that they attain similar geometries. Notably, the root mean square difference (RMSD) between these two structures is small (0.13 Å), confirming that macropa accommodates each ion effectively without significant distortion. By contrast, complexes of macropa with smaller ions like Lu^{3+} give rise to strained and asymmetric structures that reflect their poor stability.[8] These DFT calculations thus support the hypothesis that macropa would be an effective chelator for Ra^{2+}.

1.2 Preparation of ^{223}Ra

^{223}Ra was produced using an in-house microgenerator as previously described.[9] Briefly, ^{223}Ra was purified from a source of the parent isotopes ^{227}Ac and ^{227}Th. The parent isotopes were obtained as a by product of the high energy spallation of thorium targets at Los Alamos National

Laboratory (DOE), following ^{225}Ac decay (>15 half-lives). The ^{227}Ac and ^{227}Th were loaded onto an anion exchange resin (strong base, type 1, Dowex 1×8, 100–200 mesh), and each radiometal was separated based on charge discrepancy." ^{223}Ra was eluted in MeOH/HNO_3 (2N) (80:20) and concentrated until dryness. Following purification, two solutions were prepared. ^{223}Ra was redissolved in ultrapure metal-free water for chelation preparation; while [^{223}Ra]$RaCl_2$ was prepared solvated in sodium citrate (0.03 M) buffer / saline pH 6.5. All buffer formulations were prepared utilizing metal-free ultrapure water previously purified through Chelex 100 resin for demetallation.

1.3 ^{223}Ra-labeling procedures of macropa, DOTA, and EDTA

Solutions of macropa were prepared at various concentrations ranging from nM to mM (0.187; 0.935; 1.87; 9.35; 18.7; 37.4; 74.8; 374; 748; 1870; 3740 µM) in ammonium acetate (0.1 M, pH 6). Radiolabeling was conducted by adding ^{223}Ra (100 nCi, 3.7kBq /vial) in metal-free water directly to the buffered chelator solution. Reaction progress was monitored at various time points over the course of 60 min by spotting the reaction solutions on cellulose thin layer chromatography (TLC) strips coated with diglycolamide (DGA; Triskem; France). The strips were developed with a mobile phase of 0.1 M NaOH. Under these conditions, DGA coating enables a separation of structures based on charges, allowing for a differentiation of free ^{223}Ra (previously dissolved in 0.1 M NH_4OAc) remaining at the baseline ($R_f = 0$) and [^{223}Ra(macropa)] migrating with the solvent front ($R_f = 1$). Similarly, a preparation of DOTA (10 mM) or EDTA (5 mM) in NH_4OAc (0.1 M) was tentatively labeled with ^{223}Ra and migrated on TLC (Fig. S2). TLC plates were imaged on a Cyclone autoradiographic system 24 h post-development, at radioactive equilibrium, to allow time for the daughters to completely decay, ensuring that the radioactive signal measured was generated only by the parent ^{223}Ra. Quantitative radioactive signal was acquired by exposing the TLC strips to a phosphor imaging sheet for 5–10 min. Autoradiographic quantification of TLC allows for accurate quantification of activity dispersion over the chromatographic strip. Image quantification was conducted by digital light unit analysis using ImageJ software decryption with systematic tracing of TLC region of interest including lower half (unchelated) and upper half (chelated).

The radiolabeling efficiency (RL%) was calculated by integrating the area under the peaks on the radiochromatogram: dividing the counts associated with [^{223}Ra][Ra(macropa)] by the total counts integrated along the length of the TLC plate. $RL\%_{50}$ was calculated determining the ligand concentration at which half of the radioactivity was chelated by macropa (Fig. 2c in main text and

Fig S3). $RL\%_{50}$ was calculated to be identical at 5 min and 60 min post ligand addition, supporting the hypothesis of nearly instantaneous chelation of ^{223}Ra by macropa.

1.4 Serum stability of radiolabeled complexes

In vitro serum stability of [^{223}Ra][Ra(macropa)], [^{223}Ra][Ra(macropa-β-alanine)], and [^{223}Ra][Ra(macropa-DUPA)] were undertaken utilizing human serum (Sigma Aldrich). Ligands (0.1 mM) were dissolved in NH_4OAc (0.1 M) and radiolabeled with ^{223}Ra (100 nCi, 3.7 KBq) at room temperature for 30 min. RL completion (varying from 90 to 95% depending on the construct) was confirmed before undergoing serum assay. Human serum was added to each radiocomplex mixture (1:2 vol/vol) and incubated at 37 °C under gentle shaking for 12 days. To identify unchelated material upon serum challenge, we first tested aliquots of incubation utilizing DGA-coated TLC assays similar to those used for RL% assessment (see Section 1.3). However, in contrast to buffered preparations, this method led to poor separation of each radioactive entity (Fig. S4a).

Several other attempts of TLC migrations separating free ^{223}Ra from macropa-chelated entity were conducted utilizing silica coated TLCs with and without serological challenges. Two solvent systems were utilized with 80% MOPS/20% MeOH solution; as well as another migration method was conducted with 57.5 mM EDTA with and without PBS and serum challenges (Alfa Aesar, Ward Hill, MA). The stationary phase utilized was TLC plastic backed sheets with silica gel 60 (EMD Chemicals, Gibbstown, NJ). The completed TLC plates were allowed to equilibrate for 16 hours before being evaluated for compound separation on a Bioscan AR-2000 (Eckert and Ziegler, Hopkinton, MA). Similarly to DGA chromatographic migrations, weakly bound ^{223}Ra was clearly separated from macropa-chelated species in mild buffering conditions. However, upon challenges with PBS or serum, no conclusive results were recorded in regard to separation of each labeled species (Fig. S4 b, c).

Instead, radiocomplex integrities were evaluated utilizing size exclusion chromatography (SEC) (47 min elution at 1 mL/min). SEC separates molecules by mass and can disrupt weak ionic interactions between molecules and proteins in the serum mixture. This method can distinguish between proteins and their aggregates (elution volume 5–10 mL), molecular species (10–30 mL), and free ions (>30 mL). Accordingly, SEC of [^{223}Ra]$RaCl_2$ reveals the presence of a single broad peak in the radiochromatogram that begins eluting past 25 mL. For comparison, we also injected a purified sample of non-radioactive [Ba(macropa)] and a freshly radiolabeled solution of

[^{223}Ra][Ra(macropa)]. As shown in Fig. S5, [Ba(macropa)] (panel a) and [^{223}Ra][Ra(macropa)] (panel b) both elute as single peaks near 20 mL. The similarity of their elution volume confirms the incorporation of ^{223}Ra into macropa and validates our DFT studies (Section 1.1) that show that these two ions form structurally analogous complexes with this ligand. Furthermore, these chromatograms provide a clear distinction between uncomplexed and macropa-bound [^{223}Ra]Ra^{2+}.

Serum stability was evaluated by injecting aliquots (25 μL) of each solution at day 0, 1, 4, 6, and 12 of serum incubation, with day 0 corresponding to the day of mixing serum with the freshly formed radiocomplex. SEC was utilized to read serum protein stability of [^{223}Ra][Ra(macropa)] (Fig. 3 in main text), [^{223}Ra][Ra(macropa-β-alanine] (Fig. S20), and [^{223}Ra][Ra(macropa-DUPA)] (Fig. S24), and to identify urine contents upon macropa excretion (Fig. S7b). A prepacked resin column Superose 12 10/300GL was eluted with freshly prepared 50 mM Na_2HPO_4 and 150 mM NaCl buffered at pH 6.5. Compounds were separated based on molecular weight. The eluted samples were monitored at 280 nm and collected fractions (1 mL) were gamma counted at radioactive equilibrium. Gamma counting is expressed in counts per minute (CPM) and was conducted utilizing a Perkin Elmer - Wizard2 NaI gamma counter. The energy window was set to 100–450 KeV to capture the main peak at 269 KeV (abundance 13.7%).

1.5 Stability of Ba^{2+} complexes: hydroxyapatite challenge

The Ba^{2+} complexes of macropa, macropa-β-alanine, and macropa-DUPA were challenged with hydroxyapatite (HAP) as described previously,[7] with minor modifications. Briefly, ligand stock solutions were prepared in water, and their concentrations were determined either by potentiometric titration with KOH (macropa) or by UV-vis titration with standardized Ba^{2+} or La^{3+} (macropa-β-alanine and macropa-DUPA). An aliquot (10 μL) of Ba–L complex formed *in situ* was added to HAP (25 ± 0.9 mg) suspended in 500 mM Tris buffer (990 μL, pH 7.5). The final concentrations of Ba^{2+} and L were 2.5 μM and 2.8 μM, respectively. The quantity of suspended HAP corresponds to a 20,000-fold molar excess compared to the concentration of Ba–L complex. At time points of 1, 5, and 20 h, samples were centrifuged and diluted 8-fold with H_2O, and the barium content in solution was measured by graphite furnace atomic absorption spectroscopy (GFAAS) using THGA graphite tubes without end caps. Calibration standards (10.9–43.5 μg/L of barium) were prepared to match the conditions of the challenge,[7] and Tris buffer (62.5 mM) in water was used as the diluent. The furnace method is provided below. Challenges were carried out

in triplicate for each time point, with the exception of the 20 h HAP challenge for Ba-macropa-DUPA, which was replicated 6 times.

Furnace parameters for hydroxyapatite challenge experiment.

Parameters	Temperature (°C)	Ramp (s)	Hold (s)	Ar gas flow (mL/min)
Dry	110	1	20	250
Dry	140	10	5	250
Pyrolize	700	10	20	250
Atomize	2300	0	8	0
Clean	2500	1	10	250

Each sample was analyzed in triplicate and averaged. Between each sample, up to 3 measurements of diluent were made until the barium content left on the furnace was between –2.1 and 2.1 μg/L (<5% of the highest calibration standard). This quality control check prevents carryover between samples. After every 3 samples were analyzed, the highest calibration standard was re-analyzed. If the barium concentration was not within ±10% of the known concentration of the standard after 2 analyses, the instrument was re-calibrated and the data between the failed calibration check and the previous calibration check was excluded. Data from each time point were averaged and the results are reported as the percentage of barium remaining in the liquid phase, reflecting intact Ba–L complex. The uncertainties provided correspond to 1 standard deviation.

1.6 *In vivo* evaluation of radiolabeled complexes

In vivo experiments were conducted following a laboratory protocol approved by IACUC animal welfare of Washington University (DCM), conforming to the recommendations published in *Animal Welfare Act and Animal Welfare Regulations* (the "Blue Book") by the USDA animal care.

Preparation of [^{223}Ra][Ra(macropa)] for injections: 50 mM (250 μL) of chelator was first radiolabeled in ammonium acetate (0.1 M) containing saline (0.154 M NaCl). After addition of the purified ^{223}Ra source, the pH was adjusted to 6 by adding $NaHCO_3$ (0.1 M). The pH was verified using litmus paper. Upon radiolabeling completion, conducted 30 min at room temperature and verified by TLC, we then diluted the solution to 10 mM of macropa in saline for intravenous administration. Each mouse received 70 nCi ^{223}Ra for 10 mM of macropa in a 100 μL volume.

The radioactive organ distribution was undertaken comparing two groups of mice (FVB male, 9 weeks old; weights varying from 25–30g; n=4/group) administered with [^{223}Ra][Ra(macropa)] and unchelated ^{223}Ra. Each mouse received 70–80 nCi (equivalent to a human clinical dose of 55 KBq/kg) administered in a total volume of 100 μL. Each group was sacrificed at 15 min or 24 h post-administration. Selected tissues and biological fluids were collected, weighed, and gamma counted at equilibrium (including: blood; heart; lungs; liver; spleen; stomach; small intestines; cecum; urines; bladder; kidneys; muscle; fat and tibia). Injected activity dose per gram of tissue (% IA/g) were calculated normalizing to the initial dose activity administered to the tissue weight. Values were plotted with standard deviation of mean. Unpaired t-tests were calculated defining P values and statistical significances.

Approximately 0.1 mL of urine (per animal) was collected (n=3 per group) and samples were analyzed utilizing SEC for identification of excreted [^{223}Ra][Ra(macropa)] and free ^{223}Ra.

Preparation of [^{223}Ra][Ra(macropa-β-alanine)] for injections: a stock of 19 mg of macropa-β-alanine was dissolved in 200 μL of metal-free water (92.46 mM). Aliquots of macropa-β-alanine (20 μL) were labeled at room temperature for 30 min by the addition of ^{223}Ra (30 μL in metal-free water, 1 μCi or 37 KBq). The reaction pH was buffered to 6 with NH_4OAc (0.1 M; 55 μL); the overall concentration following radiolabeling was 17.6 mM. Radiolabeling completion was checked utilizing radioTLC and SEC. The solution was then dissolved with sterile saline adjusting 100 μL of injection per animal. The labeled amino-acid concentration was 2.6 mM for a dose of 80 nCi per injection (specific activity of 0.3 Ci/mol; 11.4 GBq/mol).

The biodistribution study was undertaken comparing 2 groups (n=5 for [^{223}Ra][Ra(macropa-β-alanine)] and n=4 for control [^{223}Ra]$RaCl_2$) of healthy female C57Bl/6 mice, 40 weeks old, weighing 30–35 g. Mice were sacrificed 24 h p.i. and organs were collected; weighed and gamma counted for calculation of injected administered dose per gram of tissue (%IA/g).

Preparation of [^{223}Ra][Ra(macropa-DUPA)] for injections: a stock of macropa-DUPA (2.33 mM; 130 μL) was dissolved in NH_4OAc (0.1 M). Aliquots of 10 μL were labeled with ^{223}Ra (1 μCi or 37 KBq). Following 1 h post-labeling, RL% was verified utilizing SEC (Fig. S24). A preparation of 38 nM / 70 nCi (0.2 mCi/mol; 7.4 KBq/mol) of [^{223}Ra][Ra(macropa-DUPA)] was dissolved in saline and administered in C57/Bl6, female, aged over 10 weeks old. Another cohort

received [^{223}Ra]$RaCl_2$ (n=2 per group). Mice were sacrificed 2 h p.i. Organs were weighed and gamma counted as previously described to report %IA/g (Fig. S25).

1.7 Syntheses and characterization of ligands and their cold Ba^{2+} complexes

All solvents and reagents, unless otherwise noted, were of ACS grade or higher and were purchased from commercial sources. Solvents noted as dry were obtained following storage over 3 Å molecular sieves. Deionized water (≥18 MΩ·cm) was obtained from an Elga Purelab Flex 2 water purification system and was used in all experiments. Inductively coupled plasma (ICP) standard solutions of barium and lanthanum (10,000 µg/mL) in nitric acid (2% v/v) were purchased from VWR (BDH Aristar). Macropa,[10,11] macropa-NCS,[8] Ba(macropa),[7] and macropa-DUPA[12] were prepared according to published literature procedures.

High-performance liquid chromatography (HPLC) consisted of a CBM-20A communications bus module, an LC-20AP (preparative) or LC-20AT (analytical) pump, and an SPD-20AV UV/vis detector monitoring at 270 nm (Shimadzu, Japan). Analytical chromatography was carried out at a flow rate of 1.0 mL/min using either an Ultra Aqueous C18 column, 100 Å, 5 µm, 250 mm × 4.6 mm (Restek, Bellefonte, PA) or an Epic Polar C18 column, 120 Å, 10 µm, 250 mm × 4.6 mm (ES Industries, West Berlin, NJ). Semi-preparative purification was performed using an Epic Polar preparative column, 120 Å, 10 µm, 25 cm × 20 mm (ES Industries) at a flow rate of 14 mL/min. A binary solvent system was used (A + B *or* C + D), with solvent A comprising 0.1% trifluoroacetic acid (TFA) in H_2O, solvent B comprising 0.1% TFA in CH_3CN; solvent C comprising 10 mM aq. NH_4HCO_3 (pH ~7–8); and solvent D comprising MeOH with 2% aq. NH_4HCO_3 (10 mM final concentration). The following linear-gradient HPLC methods were employed:

Method 1 (solvents A/B): 10% B (0–10 min), 10–100% B (10–40 min)
Method 2 (solvents A/B): 10% B (0–5 min), 10–100% B (5–25 min)
Method 3 (solvents C/D): 0% D (0–10 min), 0–100% D (10–45 min)
Method 4 (solvents C/D): 5% D (0–15 min), 0–100% D (15–45 min)

NMR spectra were recorded at 25 °C on a Varian Inova 600 MHz spectrometer or on a Bruker AV III HD 500 MHz spectrometer equipped with a broadband Prodigy cryoprobe. Chemical shifts are reported in parts per million (ppm). ^{1}H NMR and ^{13}C{^{1}H} NMR spectra were acquired in

DMSO-d_6 or D_2O and were referenced to the TMS internal standard (0 ppm) or to an internal standard of CH_3CN (2.06 ppm, ^{1}H NMR; 1.47 ppm, ^{13}C NMR), respectively. The splitting of proton resonances in the reported ^{1}H NMR spectra is defined as: s = singlet, d = doublet, t = triplet, q = quartet, m = multiplet, and br = broad. ^{19}F NMR spectra were referenced to an internal standard of fluorobenzene (–113.15 ppm). Quantitative ^{1}H and ^{19}F NMR spectra were acquired using a 30 s relaxation delay.

High-resolution mass spectra (HRMS) were obtained on an Exactive Orbitrap mass spectrometer in positive electrospray ionization (ESI) mode (ThermoFisher Scientific, Waltham, MA). UV/visible spectra were recorded on a Cary 8454 UV-Vis (Agilent Technologies, Santa Clara, CA) using 1-cm quartz cuvettes. Elemental analysis (EA) was performed by Atlantic Microlab, Inc. (Norcross, GA).

Synthesis of macropa-β-alanine

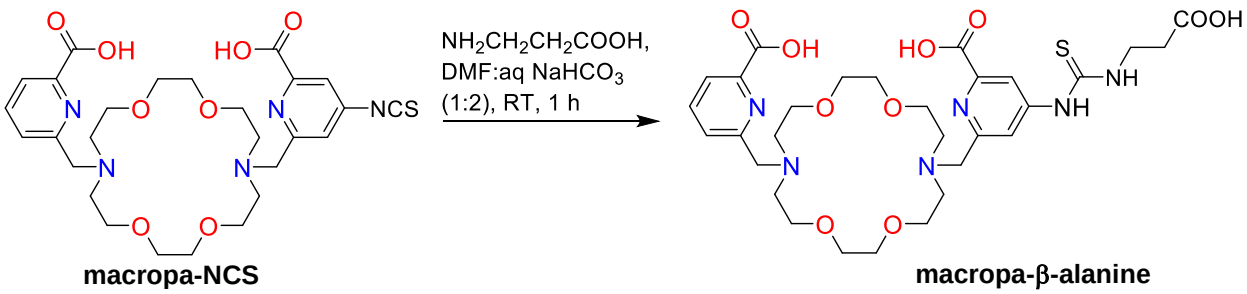

macropa-NCS **macropa-β-alanine**

Macropa-NCS was prepared from macropa-NH_2 (1.0 mmol) as described previously,[8] and the concentrate from this reaction was used directly without HPLC purification. The crude solid was suspended in DMF (18 mL), to which a solution of β-alanine (1.6875 g, 18.9 mmol) in 0.15 M aq. $NaHCO_3$ (pH 9, 0.15 M NaCl, 33 mL) was added all at once. The resulting dark-brown solution was stirred at RT for 1 h and then concentrated at 60 °C under reduced pressure. The residue was dissolved in 10% CH_3CN/H_2O containing 0.1% TFA (~11 mL), filtered through a 0.22 μm nylon membrane, and purified by preparative RP-HPLC using Method 1. Pure fractions were pooled, concentrated at 60 °C under reduced pressure, and lyophilized to give the title compound as a pale-yellow solid (0.4075 g, 38% yield). The average number of TFA counteranions per ligand was determined to be 2.9 by quantiative ^{1}H and ^{19}F NMR spectroscopy using fluorobenzene as an internal standard. ^{1}H NMR (500 MHz, D_2O) δ= 8.19 (br s, 1H), 8.12–8.08 (m, 3H), 7.77–7.73 (m, 1H), 4.80 (s, 2H, overlapping with HDO signal), 4.75 (s, 2H), 3.96–3.94 (m, 8H), 3.86 (br t, *J* =

6.5 Hz, 2H), 3.69 (s, 8H), 3.66–3.64 (m, 8H), 2.78 (t, *J* = 6.4 Hz, 2H). ^{1}H NMR (500 MHz, DMSO-d_6) δ= 13.77–12.83 (br s, 1H), 12.80–12.07 (br s, 1H), 10.53 (s, 1H), 10.11–9.33 (br s, 1H), 8.60 (br t, *J* = 5.6 Hz, 1H), 8.27 (m, 1H), 8.24 (s, 1H), 8.15–8.09 (m, 2H), 7.78 (d, *J* = 7.5 Hz, 1H), 4.70 (s, 2H), 4.64 (s, 2H), 3.90–3.80 (m, 8H), 3.71 (br q, *J* = 6.3 Hz, 2H), 3.59 (s, 8H), 3.57–3.49 (m, 8H), 2.59 (t, *J* = 6.6 Hz, 2H). ^{13}C{^{1}H} NMR (126 MHz, D_2O) δ= 180.58, 176.62, 167.66, 166.80, 163.92–163.07 (q, TFA), 151.01, 150.37, 150.00, 147.87, 147.18, 140.71, 128.68, 126.04, 120.41–113.45 (q, TFA), 119.01, 117.20, 70.55, 70.44. 64.53 (2 overlapping signals), 58.01, 57.72, 55.18, 55.02, 40.57, 33.22. ^{19}F NMR (470 MHz, DMSO-d_6) δ= –74.07. ESI-HRMS Found: *m/z* 340.14081; Calcd for $[C_{30}H_{44}N_6O_{10}S]^{2+}$: *m/z* 340.14143. Found: *m/z* 679.27420; Calcd for $[C_{30}H_{43}N_6O_{10}S]^{+}$: *m/z* 679.27559. Elem anal. Found: C, 41.89; H, 4.57; N, 8.14. Calcd for $C_{30}H_{42}N_6O_{10}S$•2.9CF_3COOH•1H_2O: C, 41.85; H, 4.60; N, 8.18. HPLC: t_R = 13.92 min (Method 2); t_R = 26.61 min (Method 3).

Synthesis of [Ba(macropa-β-alanine)]

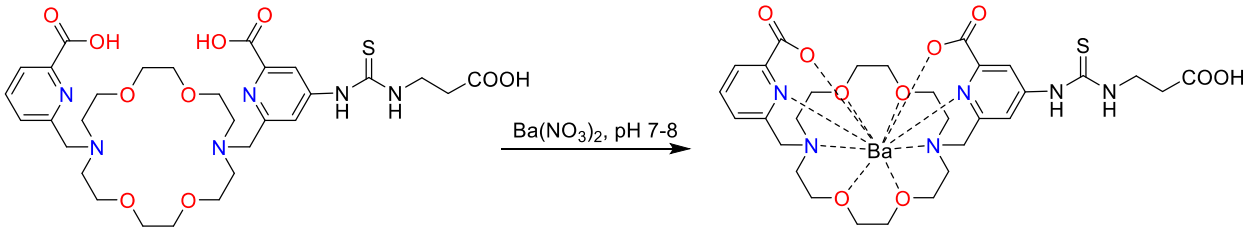

A vial was charged with macropa-β-alanine (2.175 mL of an aqueous stock solution, 0.0482 mmol) and $Ba(NO_3)_2$ (0.660 mL of ICP standard, 0.0482 mmol), and the pH of the solution was adjusted to 7–8 using 0.5 M aq. NH_4HCO_3. The solution was then purified by preparative HPLC using Method 5. The fractions containing complex were pooled, concentrated on the rotary evaporator to remove the organic solvent, and lyophilized to afford the title compound as a white solid (0.0489 g). ^{1}H NMR (500 MHz, D_2O, app pD ~6 by litmus) δ= 7.77 (t, *J* = 7.8 Hz, 1H), 7.50 (m, 2H), 7.39 (d, *J* = 7.8 Hz, 1H), 7.33 (br s, 1H), 4.87 (br t, *J* = 14.5 Hz, 2H), 4.40–4.28 (m, 2H), 4.06–3.89 (m, 6H), 3.85–3.74 (m, 2H), 3.66–3.54 (m, 4H), 3.54–3.47 (m, 2H), 3.47–3.27 (m, 6H + residual MeOH), 2.87–2.69 (m, 2H), 2.54 (t, *J* = 6.9 Hz, 2H), 2.41 (d, *J* = 13.8 Hz, 2H), 2.26 (d, *J* = 14.0 Hz, 2H). ESI-HRMS Found: *m/z* 408.08618; Calcd for $[C_{30}H_{42}BaN_6O_{10}S]^{2+}$: *m/z* 408.08623. Found: *m/z* 815.16490; Calcd for $[C_{30}H_{41}BaN_6O_{10}S]^{+}$: *m/z* 815.16518. HPLC: t_R = 25.84 min (Method 3).

Synthesis of [Ba(macropa-DUPA)]

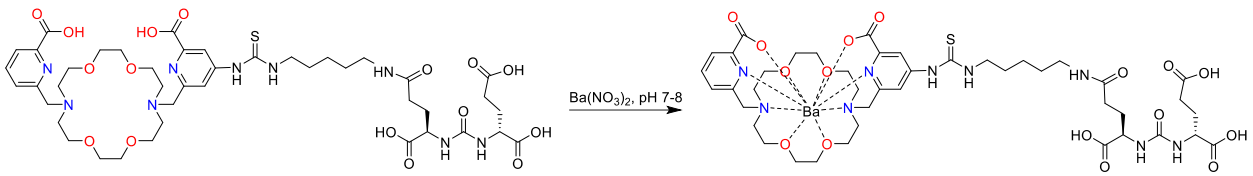

macropa-DUPA **[Ba(macropa-DUPA)]**

Macropa-DUPA (2 mL of an aqueous stock solution, 0.0048 mmol) and $Ba(NO_3)_2$ (72.3 µL of ICP standard, 0.0053 mmol), were co-mixed and the pH of the solution was adjusted to 7–8 using 0.5 M aq. NH_4HCO_3. The solution was then purified by preparative HPLC using Method 4. The fractions containing complex were pooled, concentrated on the rotary evaporator at RT to remove the organic solvent, and lyophilized to afford the title compound as a white solid (0.0083 g). ^{1}H NMR (600 MHz, D_2O, app pD ~5–6 by litmus) δ= 7.77 (t, *J* = 7.8 Hz, 1H), 7.50 (d, *J* = 7.7 Hz, 1H), 7.40 (m, 2H), 7.34 (s, 1H), 4.88 (br t, *J* = 14.6 Hz, 2H), 4.34 (m, 2H), 4.06–3.90 (m, 8H), 3.65–3.54 (m, 6H), 3.54–3.47 (m, 2H), 3.47–3.29 (m, 6H), 3.22–3.12 (m, 2H), 3.83–3.72 (br q, *J* = 13.8 Hz, 2H), 2.40 (d, *J* = 14.0 Hz, 2H), 2.34–2.23 (m, 6H), 2.11–2.00 (m, 2H), 1.90–1.80 (m, 2H), 1.66 (p, *J* = 7.2 Hz, 2H), 1.54 (p, *J* = 6.7 Hz, 2H), 1.37 (p, *J* = 8.1 Hz, 2H). ESI-HRMS Found: *m/z* 565.65631; Calcd for $[C_{43}H_{63}BaN_9O_{16}S]^{2+}$: *m/z* 565.65775. Found: *m/z* 1130.30608; Calcd for $[C_{43}H_{62}BaN_9O_{16}S]^{+}$: *m/z* 1130.30822. HPLC: t_R = 21.54 min (Method 3).

1.8 Solution thermodynamics

Protonation constants and alkaline earth (AE) stability constants of macropa-β-alanine were obtained by potentiometric titration using a Metrohm Titrando 888 titrator equipped with a Ross Orion combination electrode (8103BN, ThermoFisher Scientific), a Metrohm 806 exchange unit with an automatic buret (10 mL), and *Tiamo 2.5* software. Detailed titration setup and procedures have been reported in previous publications.[7,13] Briefly, all titration solutions were maintained at a constant ionic strength of 0.1 M using KCl and equilibrated for 25 min prior to the addition of titrant. Before every ligand or ligand-metal titration, the electrode was calibrated in terms of the hydrogen-ion concentration by titrating a solution of standardized HCl (5 mM) containing supporting electrolyte (H/KCl = 0.1 M) with standardized KOH. Data within the pH ranges of 2.3−3.2 and 10.8−11.3 were analyzed using the program Glee (version 3.0.21)[14] to obtain the

standard electrode potential (E_0) and slope factor. The H_2O ion product (pK_w = 13.78) was taken from the literature.[15] A stock solution of macropa-β-alanine was prepared in H_2O, and its exact concentration was calculated from the two sharp endpoints of its potentiometric titration curve with KOH. ICP standard solutions (1,000 μg/mL or 10,000 μg/mL, VWR BDH Aristar) of calcium, strontium, and barium in dilute HNO_3 were employed as the source of metal ions in the titrations. The exact amount of HNO_3 in the standards was determined from the endpoint of their titrations with KOH.

The protonation constants of macropa-β-alanine and the stability constants of its AE complexes were measured by adding standardized KOH to an aqueous solution (20 mL) containing ligand (0.014–0.022 mmol), mineral acid (0.1 mmol HCl for ligand titrations and 0.1 mmol HCl/NO_3 for metal-ligand titrations), and 1 M KCl (1.9 mmol) in the absence and presence of an equimolar amount of metal ion (0.014–0.022 mmol), respectively. The titration method employed a 0.1 mV min^{-1} drift limit and a maximum wait time of 180 s (ligand titrations) or 300 s (metal-ligand titrations) between additions of aliquots of base. For metal−ligand titrations, a minimum wait time of 30 s was also enforced.

The protonation and stability constants were refined using the program *Hyperquad2013*.[16] Only the proton concentration was admitted as a refinable parameter. The protonation constants, defined in eq. 1 below, were calculated from the average of six independent titrations. In the initial refinement of the data from pH 2.3 to 11.3, a high sigma value (>3) and a poor fit around the endpoints of the titration curve were obtained with a model containing only five protonation constants was used (log $K_{a1–5}$ initial estimates ≈ 7.4, 6.9, 4.3, 3.3, and 2.4). This was not a satisfactory result. Upon changing the model to reflect an additional deprotonation event in the basic region (log $K_{a1} \approx$ 11.3, $K_{a2–6} \approx$ 7.4, 6.9, 4.3, 3.3, and 2.4), the refinement proceeded to give an excellent fit and a sigma value below 2. The optimized protonation constants of macropa-β-alanine have been compiled in the main text. The errors provided correspond to 1 standard deviation. For comparison, the protonation constants of macropa are also presented.

$$K_{ai} = \frac{[H_iL]}{[H_{i-1}L][H^+]} \quad (1)$$

The first protonation constant (log K_{a1}) of macropa-β-alanine is 11.25, corresponding to a protonation event on an acidic nitrogen atom of the thiourea group ($N^- \rightarrow$ NH). The value of this protonation constant is consistent with those measured for other thiourea-containing compounds

in which the thiourea group is conjugated to an electron-withdrawing pi system.[17,18] The second and third protonation steps (log K_{a2} = 7.49, log K_{a3} = 6.90) occur on the basic amine nitrogen atoms of the macrocycle and are comparable to the corresponding protonation constants of macropa (log K_{a1} = 7.41; log K_{a2} = 6.90 (ref 7), 6.85 (ref 11).[7,11] The fourth protonation constant (log K_{a4} = 4.32) is assigned to the carboxylate group of the β-alanine moiety. The final two protonation steps measured for macropa-β-alanine, which occur at low pH, are attributed to the protonation of the picolinate arms of the ligand. These protonation constants (log K_{a5} = 3.19; log K_{a6} = 2.51) are also similar to those of macropa (log K_{a3} = 3.23 (ref 7), 3.32 (ref 11); log K_{a4} = 2.45 (ref 7), 2.36 (ref 11)).[7,11] The seventh and eighth ligand protonation constants are out of the range of measurement for our potentiometric system (log K_a < 2) and therefore could not be determined. Notably, the similarity between the protonation constants of macropa and macropa-β-alanine when comparing equivalent groups suggests that the functionalization of one picolinate arm of macropa with a thiourea-linked β-alanine moiety does not significantly affect the basicity of the diaza-18-crown-6 macrocycle or the pyridinecarboxylate arms.

To further validate the additional ligand deprotonation step that occurs under basic conditions, combined spectrophotometric-potentiometric titrations were carried out from pH 10–11.5 using an Ocean Optics dip probe (TP300-UV-Vis), DH-Mini deuterium/halogen light source, and Flame-S spectrometer. Over this pH range, the response of the electrode remains linear. Titrations were performed using 0.00420–0.00701 mmol L, 0.1 mmol HCl, and 1.9 mmol KCl in a final volume of 20 mL. The path length was 0.2 cm. A min/max wait time of 90 s was employed between additions of base; no drift limit was set. Spectra were acquired approximately 60–80 s after each aliquot of base was added; this time was determined to be sufficient for the system to reach equilibrium. Representative spectra and data fitting of a simultaneous UV-potentiometric titration of macropa-β-alanine are provided in Fig. S16. The protonation constant obtained using this method (11.36 ± 0.01) is similar to the one obtained from the potentiometric data (11.25 ± 0.11).

With the protonation constants in hand from the potentiometric titrations described above, the stepwise stability constants (eq 2 below) and protonation constants of the metal complexes (eq 3 below) were calculated from the average of three forward titrations. Hydrolysis constants for the formation of $[AE(OH)]^+$ in aqueous solution were included in the model.[19] The errors provided correspond to 1 standard deviation.

$$K_{ML} = \frac{[ML]}{[M][L]} \quad (2)$$

$$K_{MH_nL} = \frac{[MH_nL]}{[MH_{n-1}L][H]} \quad (3)$$

A comparison of the stability constants obtained for macropa-β-alanine versus those of the unfunctionalized ligand, macropa, reveals that the ligands have similar affinities for AE ions. For example, the log K_{ML} value of the Ba^{2+} complex of macropa-β-alanine (11.06) is nearly identical to that of macropa (11.11). These results suggest that conjugation of macropa to β-alanine via a thiourea linker does not appreciably alter the overall thermodynamic stability of its AE complexes. Monoprotonated complexes, or MHL species, were also detected for macropa-β-alanine bound to all three metal ions, giving rise to log K_{MHL} values ranging from 10.78 to 11.18. These constants correspond to the deprotonation of the thiourea NH of the AE complexes at high pH. Notably, the log K_{MHL} values are lower than the corresponding protonation constant of the free ligand (log K_{a1} = 11.25) and steadily decrease as the ionic radius of the AE ion decreases. We postulate that the enhanced acidity of the thiourea group upon complex formation arises from an electron-withdrawing effect originating from the metal ion. Small alkaline earth ions characterized with increased Lewis acidity were effective at polarizing the charge of the picolinate donor, thereby stabilizing the deprotonated thiourea anion. Finally, additional protonated complexes, MH_2L and MH_3L, were detected in the titrations of macropa-β-alanine with Ba^{2+} and Sr^{2+}. No additional protonated species beyond MHL could be reasonably modeled for Ca^{2+} titrations.

An alternative strategy for the refinement of the titration data was also explored, in which the deprotonation of the thiourea group at high pH was ignored. This approach was achieved by excluding all data points collected above pH 9 and removing the high protonation constant from the model. Shown in Table S4, the protonation constants calculated using this strategy were nearly identical to the corresponding protonation constants obtained when the full dataset (pH 2.3–11.3) was modeled, although a slight systematic decrease in protonation constants can be noted. AE stability constants calculated using this strategy, however, experienced more significant deviations from the stability constants modeled using the full dataset. Notably, the stability constants obtained for the Ba^{2+}, Sr^{2+}, and Ca^{2+} complexes of macropa-β-alanine are 0.03, 0.41, and 0.54 log K units lower, respectively, than that obtained when the full pH dataset is refined. These results suggest

that high pH data is important for refining the stability constants of the more Lewis acidic ions with this ligand.

1.9 X-ray diffraction

Single crystals of [Ba(macropa-β-alanine)(DMSO)] suitable for X-ray diffraction were grown from a solution of [Ba(macropa-β-alanine)] in DMSO-d_6 upon standing overnight. Low-temperature X-ray diffraction data were collected on a Rigaku XtaLAB Synergy diffractometer coupled to a Rigaku Hypix detector with Cu Kα radiation (λ = 1.54184 Å) from a PhotonJet micro-focus X-ray source at 100 K. The diffraction images were processed and scaled using the *CrysAlisPro* software (2015, Rigaku OD, The Woodlands, TX). The structure was solved through intrinsic phasing using SHELXT[20] and refined against F^2 on all data by full-matrix least squares with SHELXL[21] following established refinement strategies.[22] Visual analysis of the reflections on the data frames showed no obvious signs of non-merohedral twinning. The value of $|E^2-1|$ = 0.869 falls almost exactly in between the theoretical expectations for centrosymmetric (0.968) and noncentrosymmetric (0.736) space groups. As such, an attempt was made to solve the structure in the centrosymmetric space group Pbcm. This solution was unsuccessful; we were not able to definitively assign the structure of the main molecule. In the non-centrosymmetric space group *P*ca2_1, we were able to unequivocally establish the general connectivity and framework of the molecule using the intrinsic phasing method of SHELXT. The racemic twin law: -1 0 0 0 -1 0 0 0 -1 was applied, and the twin component refined to a value of 0.372. After application of the twin law, we were able to locate and assign most of the disordered components of the structure. The crystallographic occupancies of the two disordered components refined close to 50%. This value could suggest that the symmetry of the crystal system was incorrect. Searches for higher symmetry were carried out using the program *Platon*.[23] Attempts to solve the structure in P1 or P$\bar{1}$, to check for pseudosymmetry, were unsuccessful, as the disorder in the molecule was not resolved. The fact that the fractional component of the twin law refines to ~37% instead of 50% suggests that the structure is best described as being a racemic twin of a non-centrosymmetric crystal.

Given the results described above, the structure was refined in the *P*ca2_1 space group with the racemic twin law applied and disorder modeled with appropriate restraints. All non-hydrogen atoms were refined anisotropically. One of the nitrogen atoms of the disordered β-alanine group (N6B) gave an unrealistic thermal ellipsoid and an unstable refinement. In this case, the thermal

ellipsoid of N6B was constrained to be equal to that of N6A using the EADP command. The thermal ellipsoids of several carbon atoms in the macrocyclic core and the methyl groups of the coordinated DMSO molecule are rather large. Although we tried to model these atoms as being disordered about two positions, these attempts were unsuccessful. Thus, the atoms with their elongated thermal ellipsoids were left as is. The abnormal shape of these ellipsoids generated two B-level alerts for the DMSO methyl groups and two C-level alerts for the macrocycle carbons. All hydrogen atoms bound to carbon were included in the model at geometrically calculated positions and refined using a riding model (HFIX 137 or 33). The isotropic displacement parameters of all hydrogen atoms were fixed to 1.2 times the U_{eq} value of the atoms that they are linked to. Due to the significant twinning and disorder, we were unable to locate hydrogen atoms attached to acidic heteroatoms directly on the difference Fourier map. Short intermolecular contacts between N5 and N6 of the thiourea group and O2 of a picolinate group in neighboring molecules, however, support the presence of hydrogen atoms on the two thiourea nitrogen atoms. As such, the thiourea protons were placed in calculated positions using the HFIX 43 command. Additional hydrogen-bonding interactions are observed between carboxylate groups of neighboring picolinate and β-alanine moieties. No counteranion or solvent-accessible voids were identified during the refinement. Based on these hydrogen-bonding interactions in conjunction with the neutral charge of the complex, we postulate that one carboxylate group of the ligand is protonated. Because we could not conclusively locate these hydrogen atoms on the Fourier map, they were not included in the final model. Their lack of inclusion generated two additional B-level alerts. In the finalized structure, there are several large residual electron density peaks (Q3-Q7) corresponding to ≤ 2 e^{-} located near the sulfur atoms of the disordered β-alanine groups. These peaks could not be definitively assigned, generating a B-level alert for the ratio of the maximum and minimum density. The last B-level alert was generated by the low bond precision in the C–C bonds, which arises from the high degree of twinning and disorder in the structure. Crystallographic data collection and refinement parameters, interatomic distances, and interatomic angles are collected in Tables S5–S10.

2. SUPPORTING FIGURES, SCHEMES, AND TABLES

2.1 DFT calculations

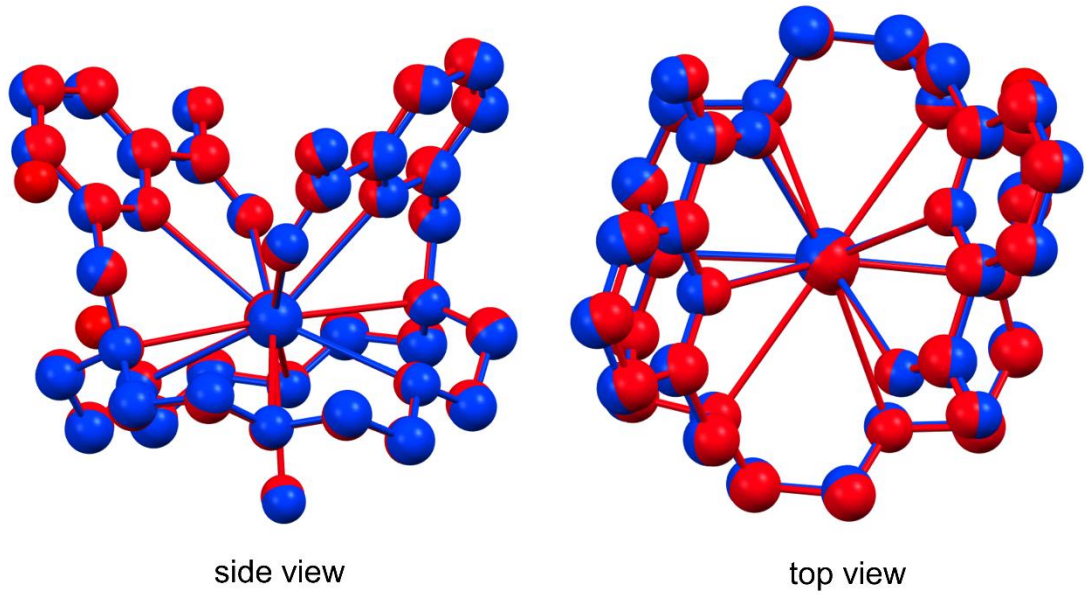

Fig. S1. Overlay of the DFT structures of [Ba(macropa)(OH_2)]·2H_2O (blue) and [Ra(macropa)(OH_2)]·2H_2O (red) optimized at the TPSSh/TZVP/LC RECP level of theory (RMSD = 0.13 Å).

Table S1. Interatomic distances (Å) of the metal coordination environments of [M(macropa)(H_2O)] calculated at the TPSSh/TZVP/LC RECP level of theory.[a]

M	M–N_{py}	M–N_{py}	M–O_{COO}	M–O_{COO}	M–O_C	M–O_C	M–O_C	M–O_C	M–N_{AM}	M–N_{AM}
Ba	2.867	2.865	2.660	2.651	2.908	2.912	3.135	3.146	3.049	3.053
Ra	2.923	2.926	2.730	2.738	2.956	2.960	3.135	3.143	3.073	3.077

[a]N_{PY} = pyridyl nitrogen atoms, O_{COO} = carboxylate oxygen atoms, O_C = crown oxygen atoms, N_{AM} = amine nitrogen atoms.

Table S2. DFT optimized coordinates of [Ra(macropa)(OH_2)]·$2H_2O$.

[Ra(macropa)(OH_2)]·$2H_2O$			0 imaginary frequencies	
Center Number	Atomic Number	X	Y	Z
1	88	-0.003446	-0.016581	-0.001465
2	8	1.028353	1.240364	2.467161
3	6	-0.01937	1.784316	3.272614
4	6	-0.969761	0.6603	3.667397
5	7	-1.733584	0.083181	2.540906
6	6	-2.962253	0.859042	2.29061
7	6	-3.592565	0.643549	0.919696
8	8	-2.82475	1.366799	-0.071238
9	6	-3.280414	1.107478	-1.420845
10	6	-2.348186	1.768773	-2.416974
11	8	-1.151338	0.996236	-2.534681
12	6	-0.155879	1.598772	-3.365254
13	6	0.90357	0.555568	-3.701162
14	7	1.713811	0.114101	-2.546406
15	6	2.85795	1.019924	-2.333809
16	6	3.504649	0.935743	-0.956244
17	8	2.666129	1.627571	0.000018
18	6	3.148207	1.487535	1.357742
19	6	2.156293	2.106323	2.322481
20	1	2.652354	2.222539	3.296355
21	1	1.83783	3.095255	1.973046
22	1	4.108947	2.010093	1.451513
23	1	3.281722	0.423035	1.567765
24	1	3.630301	-0.095564	-0.614246
25	1	4.483751	1.432749	-0.992014
26	1	2.507213	2.044321	-2.48982
27	1	3.642253	0.831201	-3.088202
28	6	2.19046	-1.276968	-2.722148
29	1	2.76751	-1.537623	-1.829013
30	1	2.852927	-1.357283	-3.600326
31	6	1.065502	-2.28289	-2.847808
32	7	0.009471	-2.109186	-2.042772
33	6	-1.009358	-2.979324	-2.086317
34	6	-0.993847	-4.088297	-2.933532
35	6	0.104323	-4.280129	-3.760676
36	6	1.149333	-3.359052	-3.729402
37	1	2.01444	-3.472772	-4.373528

38	1	0.148289	-5.131519	-4.431907
39	1	-1.844759	-4.757355	-2.920474
40	6	-2.222431	-2.710668	-1.180422
41	8	-2.124195	-1.682071	-0.425428
42	8	-3.175975	-3.491666	-1.27414
43	1	0.385679	-0.317023	-4.100719
44	1	1.545068	0.954847	-4.504499
45	1	0.263896	2.475931	-2.855328
46	1	-0.615039	1.935834	-4.305168
47	1	-2.855386	1.803006	-3.391408
48	1	-2.111932	2.794119	-2.110048
49	1	-4.288276	1.524398	-1.543316
50	1	-3.303481	0.025173	-1.573776
51	1	-3.609927	-0.411166	0.63074
52	1	-4.617025	1.039674	0.931547
53	1	-2.718437	1.919891	2.399827
54	1	-3.725282	0.626429	3.054344
55	6	-2.07262	-1.33604	2.793611
56	1	-2.624931	-1.698538	1.920962
57	1	-2.721373	-1.431968	3.680331
58	6	-0.857759	-2.223353	2.963761
59	7	0.180545	-1.989759	2.150837
60	6	1.274499	-2.76068	2.233376
61	6	1.356648	-3.827446	3.129466
62	6	0.278051	-4.081056	3.965646
63	6	-0.845931	-3.261408	3.893807
64	1	-1.69942	-3.424446	4.542869
65	1	0.309548	-4.902105	4.674332
66	1	2.264645	-4.416559	3.14523
67	6	2.461758	-2.425058	1.315541
68	8	2.275154	-1.444397	0.515071
69	8	3.480721	-3.11313	1.443845
70	1	-0.366588	-0.13527	4.106454
71	1	-1.646361	1.033601	4.454308
72	1	-0.525248	2.589019	2.722019
73	1	0.405649	2.213098	4.190824
74	8	-0.124481	3.139012	-0.131766
75	1	-0.918365	3.688663	0.015719
76	1	0.618367	3.757353	-0.271886
77	8	2.381426	4.334235	-0.393752

78	1	2.625121	3.380455	-0.351318
79	1	2.839051	4.705013	-1.156772
80	8	-2.723684	4.10461	0.187408
81	1	-3.187028	4.481541	0.943883
82	1	-2.901537	3.135636	0.198005

Zero-point correction=	0.666391 (Hartree/Particle)
Thermal correction to Energy=	0.71199
Thermal correction to Enthalpy=	0.712934
Thermal correction to Gibbs Free Energy=	0.588253
Sum of electronic and zero-point Energies=	-2085.6895
Sum of electronic and thermal Energies=	-2085.6439
Sum of electronic and thermal Enthalpies=	-2085.6429
Sum of electronic and thermal Free Energies=	-2085.7676

Table S3. DFT optimized coordinates of [Ba(macropa)(OH_2)]·$2H_2O$.

[Ba(macropa)(OH_2)]·$2H_2O$			0 imaginary frequencies	
Center Number	Atomic Number	X	Y	Z
1	56	-0.06525	0.159963	-0.044074
2	8	0.952963	1.400438	2.381356
3	6	-0.083077	1.930872	3.209881
4	6	-1.02687	0.801451	3.59648
5	7	-1.800274	0.246939	2.465953
6	6	-3.025209	1.036254	2.244166
7	6	-3.672448	0.837486	0.881375
8	8	-2.891657	1.540179	-0.110932
9	6	-3.348123	1.27474	-1.45646
10	6	-2.406713	1.919774	-2.451309
11	8	-1.202575	1.155411	-2.532556
12	6	-0.219115	1.744165	-3.386301
13	6	0.835828	0.697468	-3.715852
14	7	1.653901	0.27854	-2.558941
15	6	2.793907	1.194624	-2.374566
16	6	3.453767	1.126499	-1.004843
17	8	2.605897	1.801959	-0.048583
18	6	3.086499	1.660473	1.306915
19	6	2.083942	2.265598	2.2663
20	1	2.565615	2.366699	3.249141
21	1	1.771512	3.26004	1.926815
22	1	4.041992	2.19183	1.407576
23	1	3.227894	0.596654	1.513685
24	1	3.597583	0.098113	-0.663326
25	1	4.423276	1.641981	-1.047057
26	1	2.433952	2.21494	-2.536067
27	1	3.569131	1.002863	-3.137593
28	6	2.141926	-1.108416	-2.726794
29	1	2.739375	-1.351585	-1.842945
30	1	2.783785	-1.193783	-3.619769
31	6	1.023153	-2.122792	-2.811839
32	7	-0.029393	-1.925487	-2.008238
33	6	-1.043346	-2.802302	-2.019862
34	6	-1.028698	-3.938199	-2.829449
35	6	0.066246	-4.152973	-3.65537
36	6	1.106725	-3.226908	-3.658794
37	1	1.969389	-3.357183	-4.303013

38	1	0.110538	-5.025406	-4.298968
39	1	-1.877303	-4.609151	-2.789932
40	6	-2.249702	-2.501542	-1.120843
41	8	-2.145945	-1.441329	-0.411217
42	8	-3.204818	-3.284589	-1.172022
43	1	0.314852	-0.181856	-4.09605
44	1	1.47174	1.082733	-4.530554
45	1	0.205314	2.63082	-2.897393
46	1	-0.691883	2.063638	-4.325606
47	1	-2.898279	1.928301	-3.434427
48	1	-2.183179	2.953705	-2.163889
49	1	-4.351797	1.700285	-1.586189
50	1	-3.380077	0.191881	-1.601613
51	1	-3.716052	-0.216433	0.594598
52	1	-4.686889	1.259102	0.899999
53	1	-2.770477	2.09393	2.35901
54	1	-3.778431	0.802774	3.017398
55	6	-2.152512	-1.169115	2.71105
56	1	-2.729094	-1.514914	1.848049
57	1	-2.778705	-1.26629	3.61386
58	6	-0.944545	-2.069976	2.839188
59	7	0.090804	-1.812394	2.03025
60	6	1.178085	-2.595576	2.079566
61	6	1.258624	-3.695012	2.934331
62	6	0.182772	-3.971623	3.766954
63	6	-0.93464	-3.141471	3.731028
64	1	-1.786041	-3.321456	4.378286
65	1	0.211911	-4.818215	4.445006
66	1	2.162662	-4.290282	2.922575
67	6	2.358212	-2.228252	1.170102
68	8	2.167171	-1.210925	0.417199
69	8	3.376698	-2.923698	1.254423
70	1	-0.418796	-0.001599	4.014481
71	1	-1.696792	1.159441	4.396297
72	1	-0.596008	2.745103	2.680438
73	1	0.355766	2.343559	4.12897
74	8	-0.192617	3.242827	-0.179233
75	1	-0.982784	3.795442	-0.023179
76	1	0.548155	3.862666	-0.323385
77	8	2.287186	4.497205	-0.448958

78	1	2.548708	3.548169	-0.400736
79	1	2.732937	4.870647	-1.217687
80	8	-2.769055	4.269026	0.151527
81	1	-3.221969	4.646194	0.914153
82	1	-2.960563	3.302255	0.155024

Zero-point correction=	0.667196 (Hartree/Particle)
Thermal correction to Energy=	0.712483
Thermal correction to Enthalpy=	0.713427
Thermal correction to Gibbs Free Energy=	0.589977
Sum of electronic and zero-point Energies=	-2087.1267
Sum of electronic and thermal Energies=	-2087.0814
Sum of electronic and thermal Enthalpies=	-2087.0805
Sum of electronic and thermal Free Energies=	-2087.2039

2.2 Ligand radiolabeling

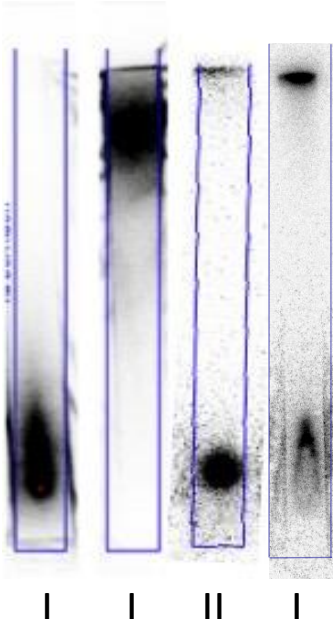

Fig. S2. TLC autoradiographic readings of [^{223}Ra][Ra(macropa)] (10 mM), DOTA (10 mM) and EDTA (5mM) migrated on DGA-coated TLC using a NaOH (0.1 M) mobile phase. I. [^{223}Ra]$RaCl_2$ migration ($R_f \approx 0$); II. [^{223}Ra][Ra(macropa)] ($R_f \approx 1$); III. ^{223}Ra tentatively chelated with DOTA showing unsuccessful radiolabeling (85% remained unchelated); IV. ^{223}Ra partially chelated with EDTA (65% remained unchelated).

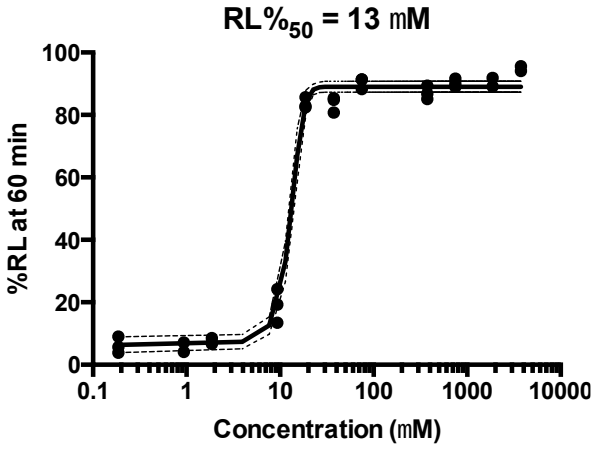

Fig. S3. Radiolabeling efficiencies (RL%) recorded at 60 min as a function macropa concentration (n = 3). RL at 50% was correlated with 13 µM of macropa concentration. This value is identical to the one calculated at 5 min post macropa mixing, demonstrating instantaneous complexation of ^{223}Ra by macropa.

2.3 Serum stability of radiolabeled complexes

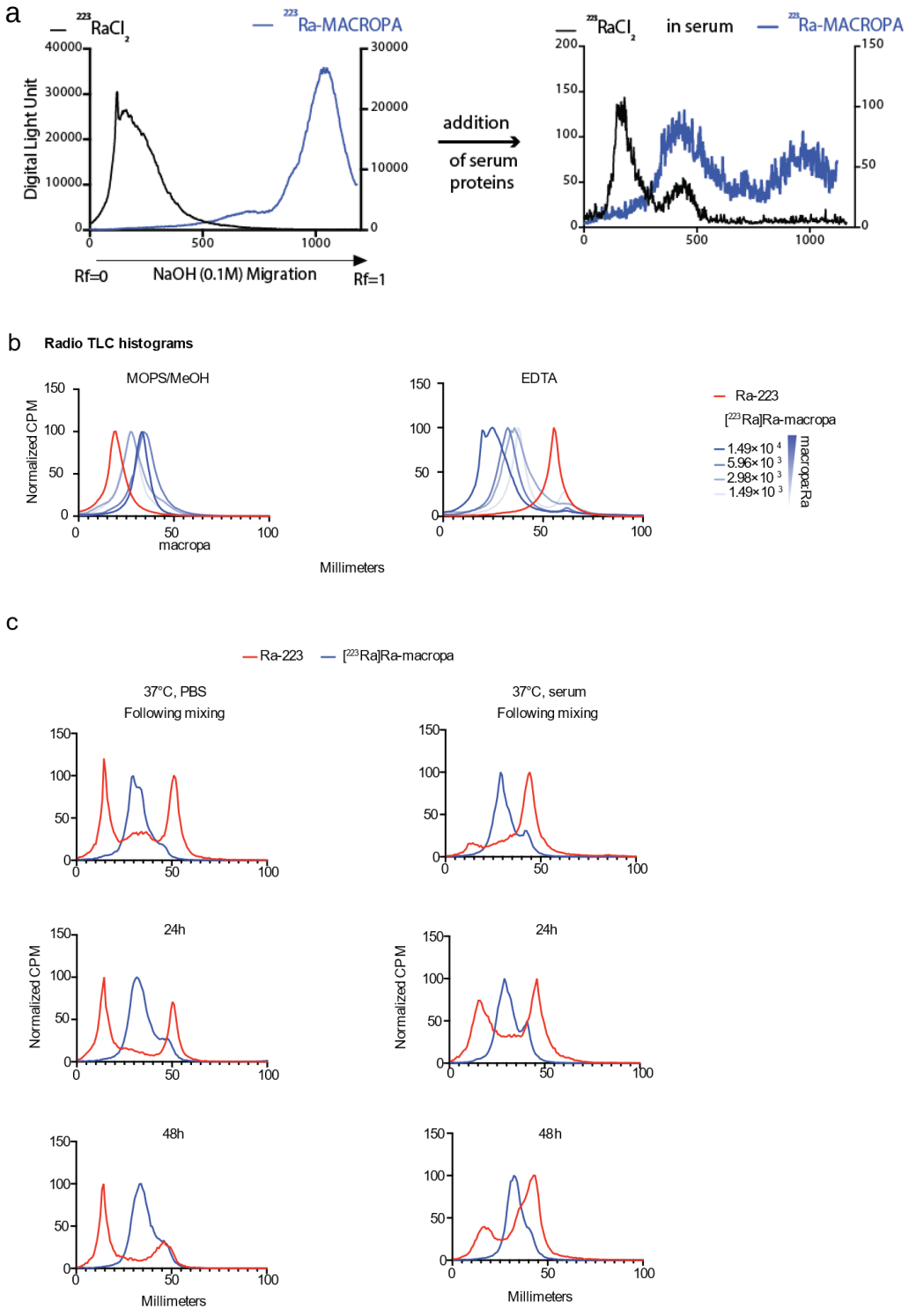

Fig. S4. Overlaid TLC profiles of pure [^{223}Ra]$RaCl_2$ and labeled macropa in PBS (left panel) and in human serum (right panel). a. In contrast to buffered preparations, [^{223}Ra]$RaCl_2$ (black trace) and [^{223}Ra][Ra(macropa)] (blue trace) mixed in serum were poorly separated, questioning the suitability of the DGA-coated chromatographic technique to detect ^{223}Ra decomplexation in serum. Weak ionic interactions of [^{223}Ra]Ra^{2+} or [^{223}Ra][Ra(macropa)] with proteins may occur and result in the inability of TLC to clearly separate each species. b. Silica-coated TLCs of [^{223}Ra]$RaCl_2$ and [^{223}Ra][Ra(macropa)] migrated utilizing mobile phase 1 (MOPS/MeOH:80:20) or mobile phase 2 (EDTA- 50 mM); c. Similarly, PBS and serum challenges of [^{223}Ra][Ra(macropa)] were evaluated utilizing EDTA migration; leading to a challenging readout of the results. Alternatively, size exclusion chromatography was considered, demonstrating efficient separation of radioconstructs from proteins.

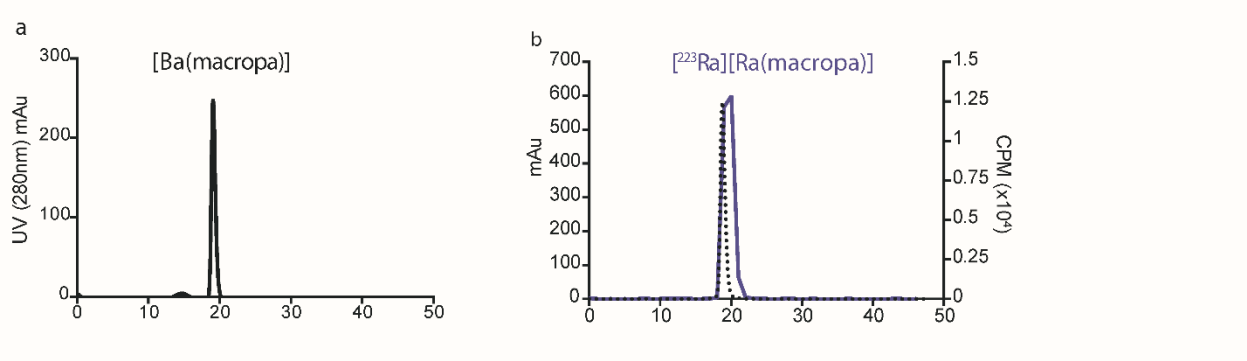

Fig. S5. Size exclusion chromatography (SEC) of a) [Ba(macropa)] detected at 280 nm (mAu); b) [^{223}Ra][Ra(macropa)] detected by both UV (black dashed line) and gamma counting - counts / min (CPM) (purple solid line) within 1 h following radiolabeling in buffer, in the absence of serum.

2.4 Hydroxyapatite challenge

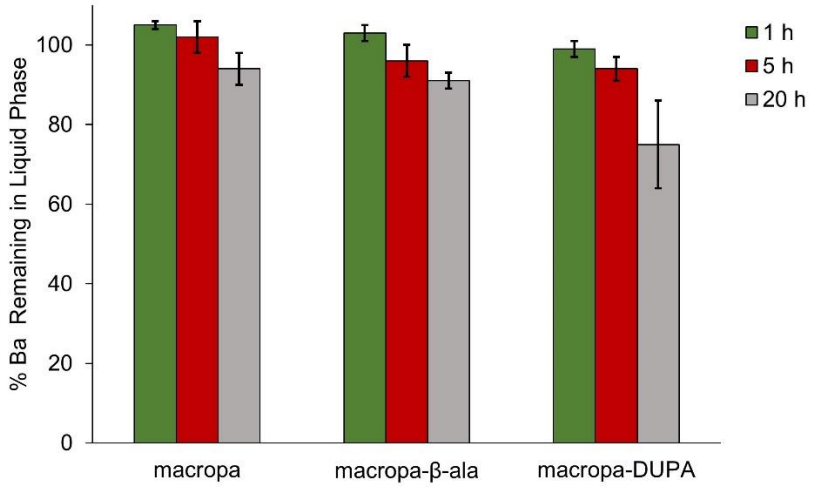

Fig. S6. Hydroxyapatite challenge. Barium complexes of macropa, macropa-β-alanine (ala), and macropa-DUPA were stirred at RT in the presence of HAP (25 mg). The suspensions were filtered after 1, 5, or 20 h, and the filtrate was analyzed by GFAAS to determine the amount of barium remaining in the liquid phase, reflecting intact Ba–L complex. Under these conditions, unchelated barium ($Ba(NO_3)_2$) is quantitatively adsorbed by HAP within 10 minutes in the absence of ligand.

2.5 In vivo biodistribution of [^{223}Ra][Ra(macropa)]

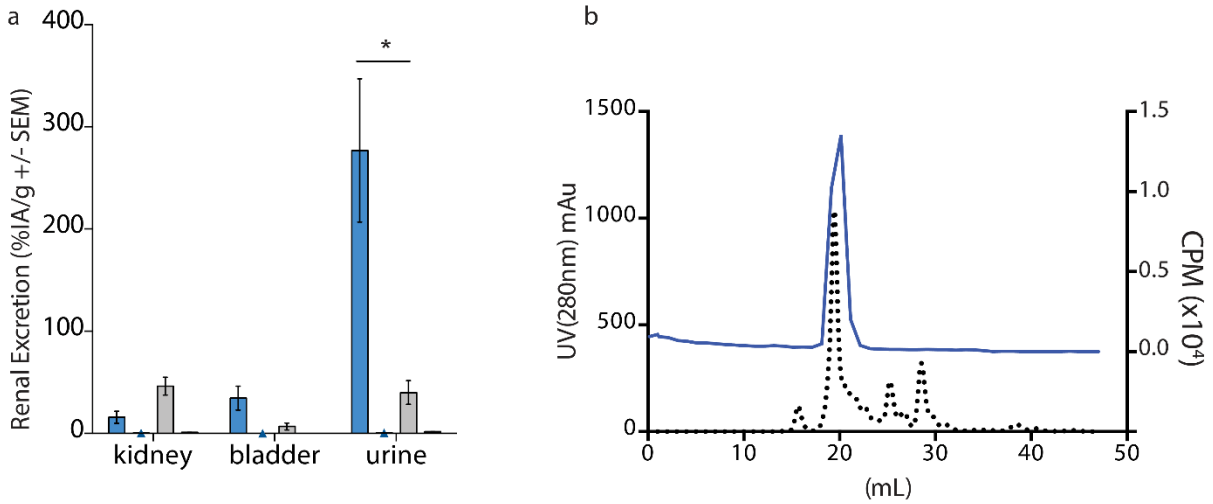

Fig. S7. *In vivo* evaluation of [^{223}Ra][Ra(macropa)]. a) Comparative renal excretion shows nearly complete clearance of the chelated radionuclide (**p*=0.01). b) SEC of urine collected from [^{223}Ra][Ra(macropa)]-treated mice, indicating the excretion of the intact complex.

2.6 Characterization of macropa-β-alanine

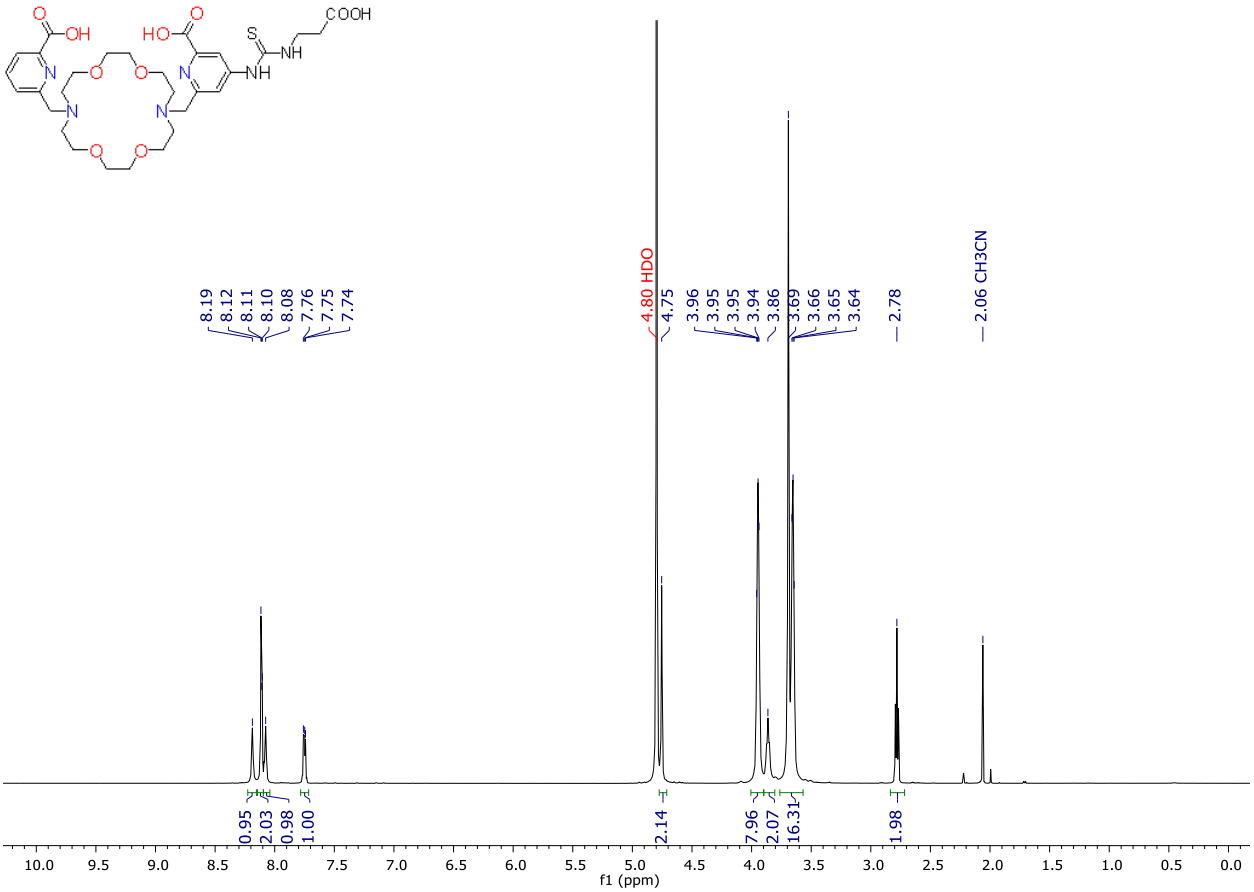

Fig. S8. ^{1}H NMR spectrum of macropa-β-alanine. 500 MHz, D_2O. CH_3CN was added as an internal standard.

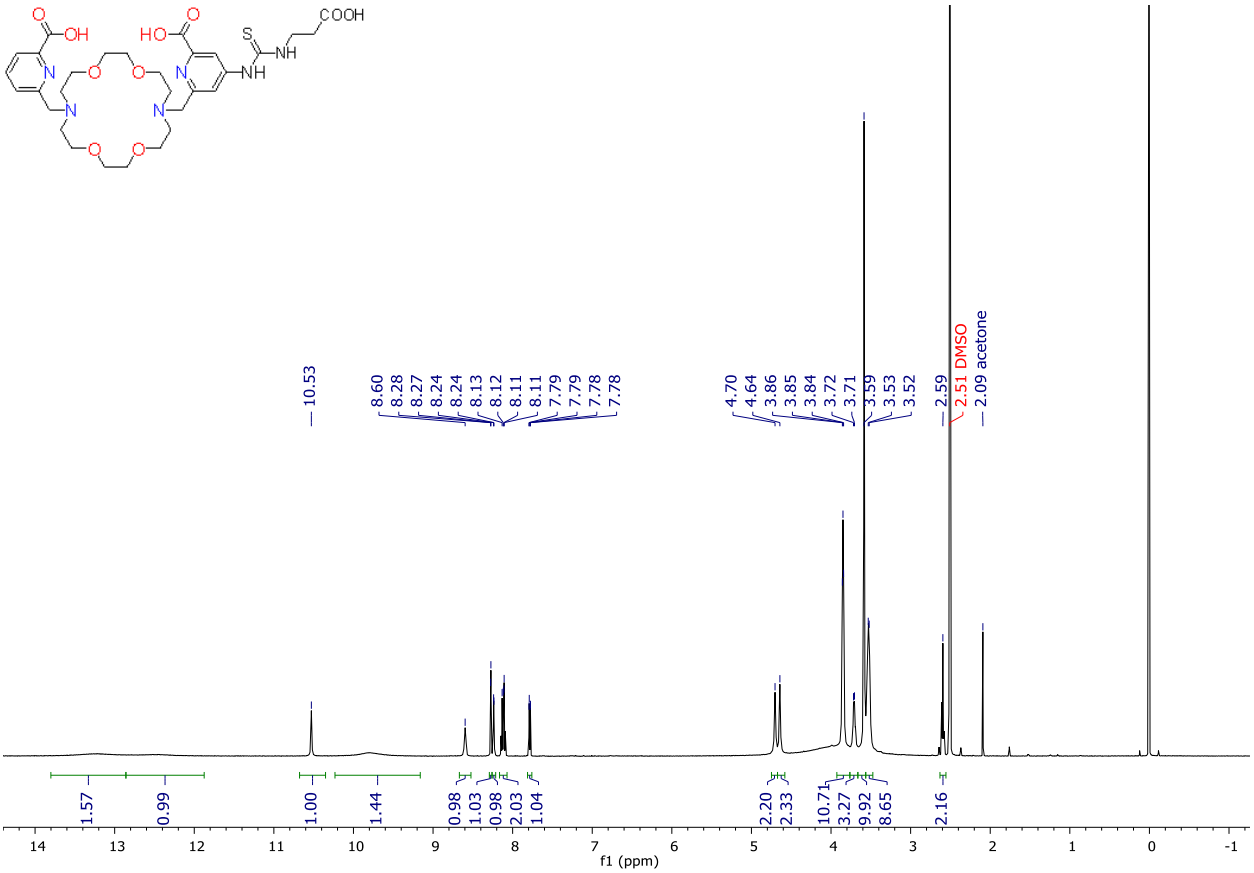

Fig. S9. ^{1}H NMR spectrum of macropa-β-alanine. 500 MHz, DMSO-d_6.

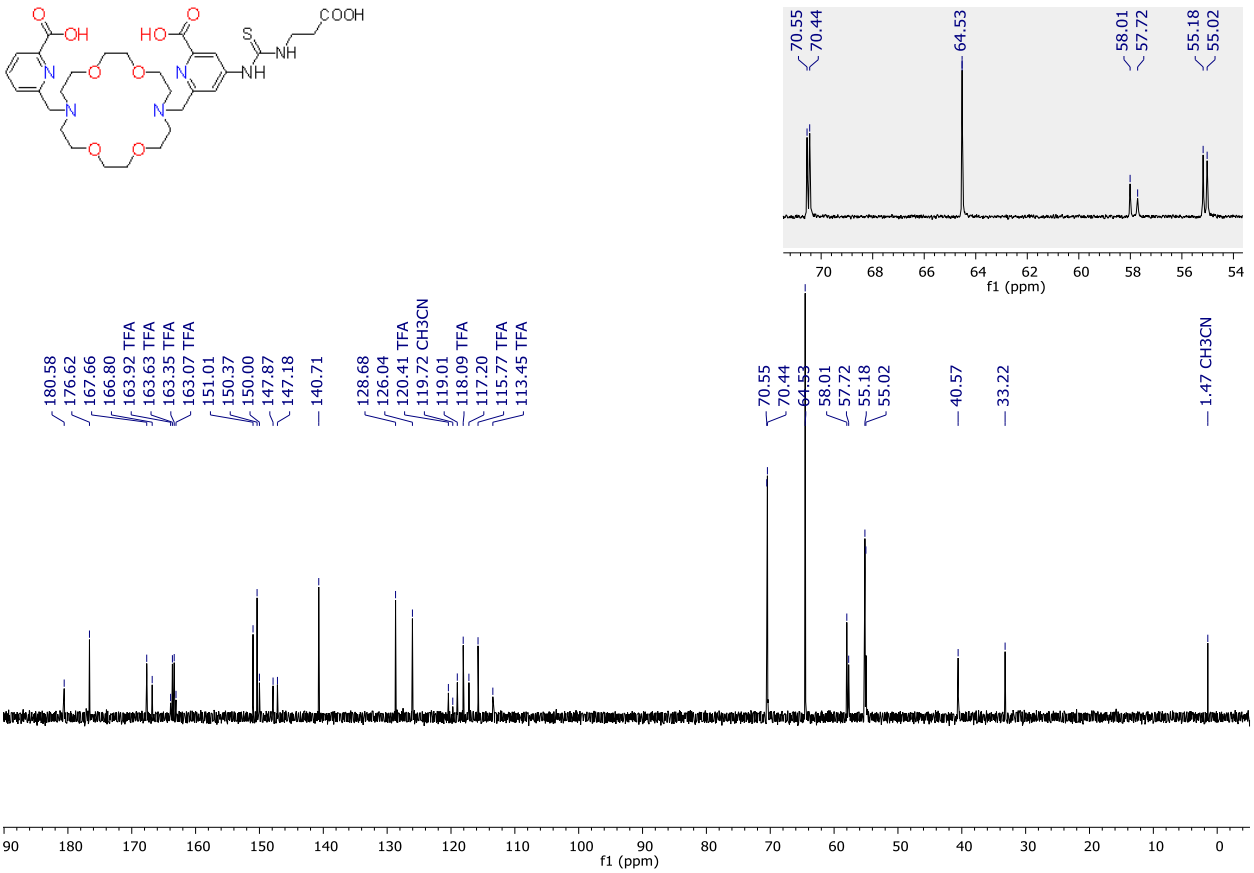

Fig. S10. $^{13}C\{^{1}H\}$ NMR spectrum of macropa-β-alanine. 126 MHz, D_2O. CH_3CN was added as an internal standard. Based on ^{13}C spectra of similar compounds,[7] two carbon signals overlap at 64.53 ppm.

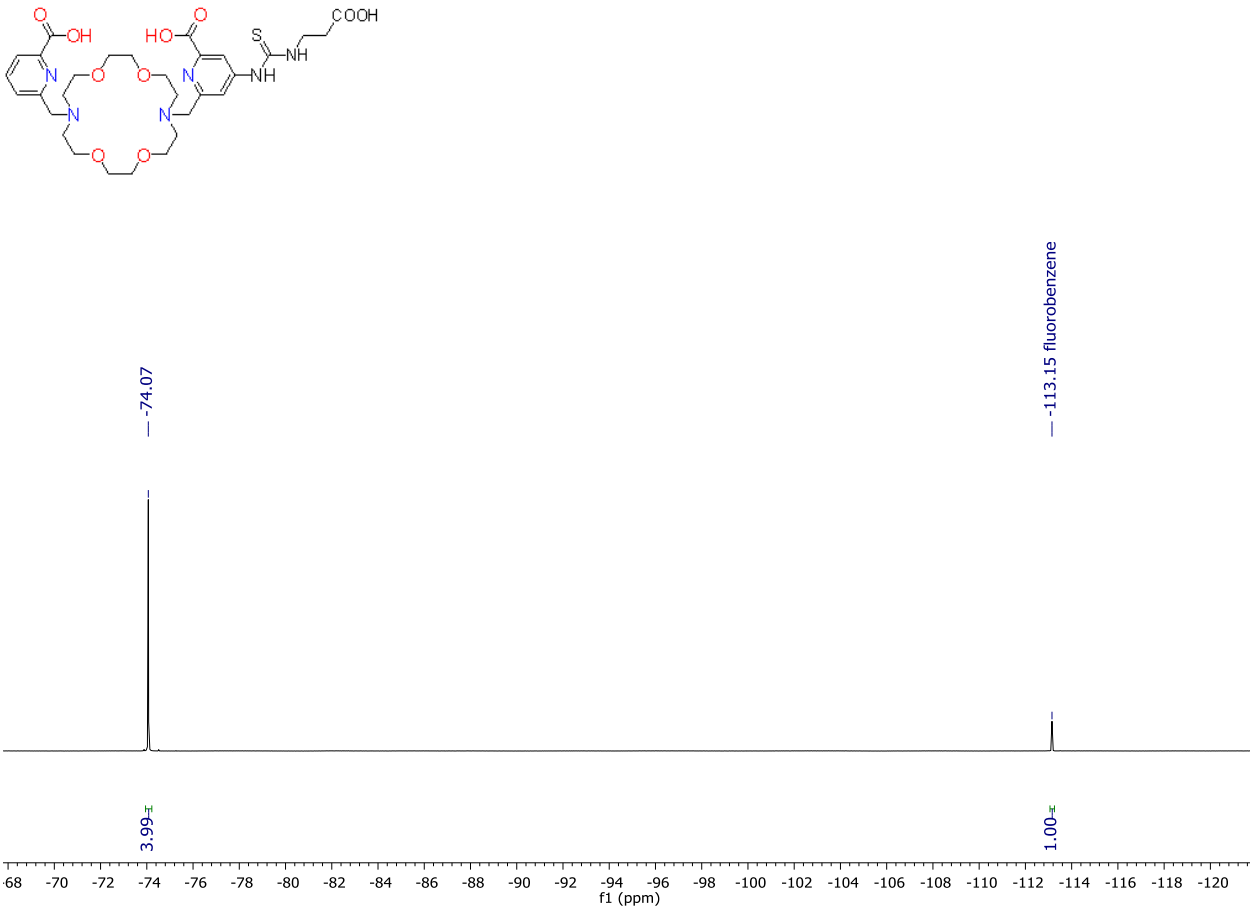

Fig. S11. ^{19}F NMR spectrum of macropa-β-alanine. 470 MHz, DMSO-d_6. Fluorobenzene was added as an internal standard.

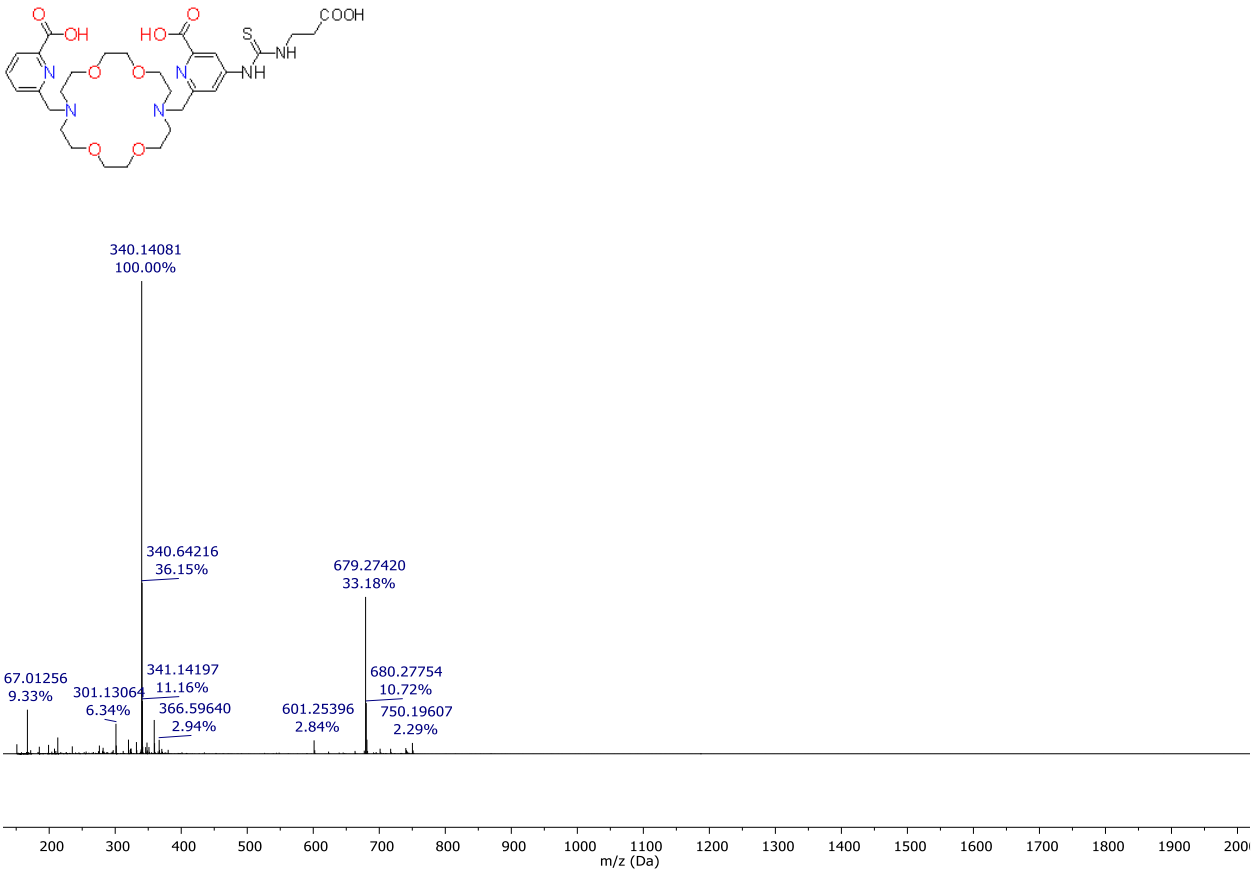

Fig. S12. ESI-HRMS of macropa-β-alanine. The sample was diluted in CH_3CN:H_2O (7:3) containing 0.1% formic acid and analyzed using a mobile phase of CH_3CN:H_2O (1:1) containing 0.1% formic acid. Two ions were observed, corresponding to $[M+H]^+$ (*m/z* 679.27420) and $[M+2H]^{2+}$ (*m/z* 340.14081).

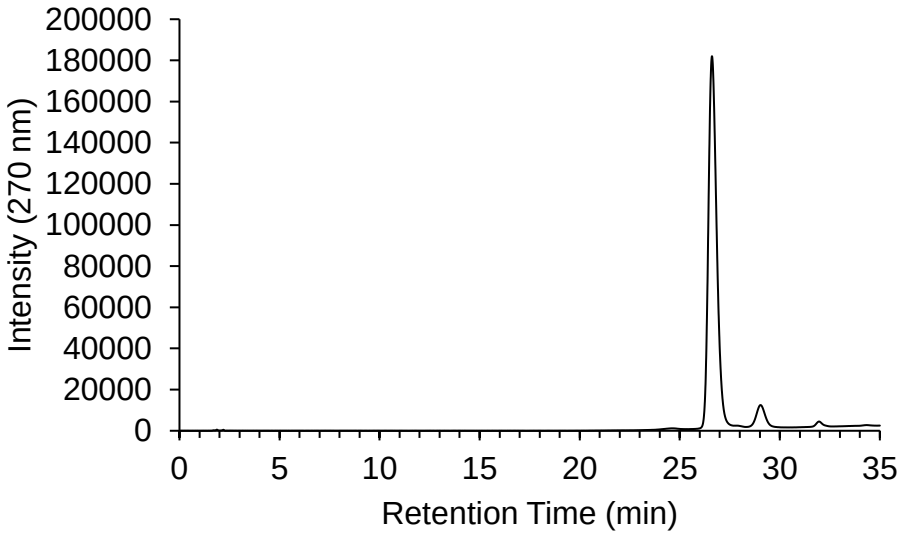

Fig. S13. HPLC chromatogram of macropa-β-alanine. Retention time (t_R) = 26.61 min using a binary MeOH/H_2O mobile phase containing 10 mM NH_4HCO_3 (program: 0% MeOH for 10 min followed by a linear gradient to 100% MeOH over 35 min).

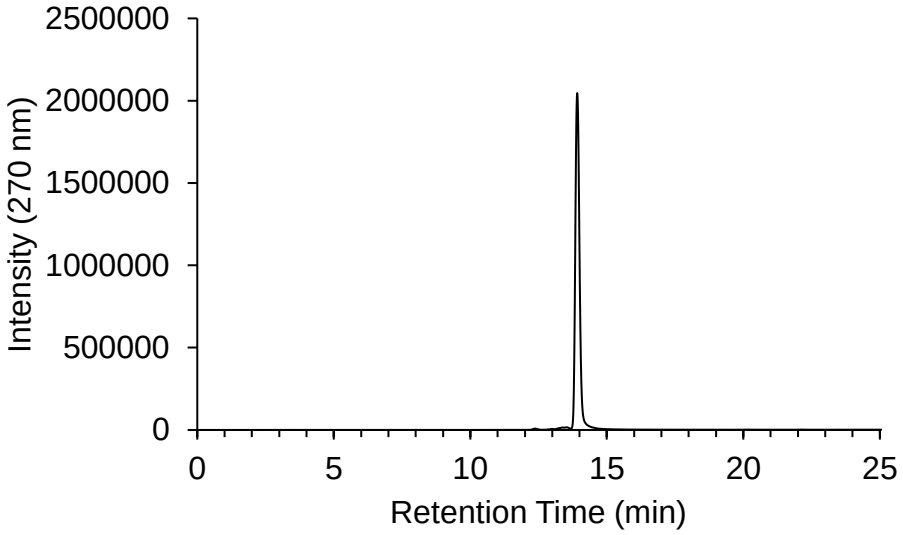

Fig. S14. HPLC chromatogram of macropa-β-alanine utilizing an alternative solvent method. Retention time (t_R) = 13.92 min using a binary CH_3CN/H_2O mobile phase containing 0.1% TFA (program: 10% CH_3CN for 5 min followed by a linear gradient to 100% CH_3CN over 20 min).

2.7 Solution thermodynamics

Table S4. Protonation constants and AE stability constants of macropa-β-alanine calculated when data at high pH (≥ pH 9) are excluded from the refinements.

	macropa-β-alanine $^{4-}$
log K_{a1}	7.41(0.02)
log K_{a2}	6.82(0.01)
log K_{a3}	4.20(0.01)
log K_{a4}	3.15(0.02)
log K_{a5}	2.43(0.04)
log K_{a6}	
log K_{BaL}	11.03(0.06)
log K_{BaHL}	4.47(0.03)
log K_{BaH2L}	3.43(0.02)
log K_{BaH3L}	2.75(0.13)
log K_{SrL}	9.17(0.06)
log K_{SrHL}	4.45(0.03)
log K_{SrH2L}	
log K_{CaL}	5.61(0.02)
log K_{CaHL}	

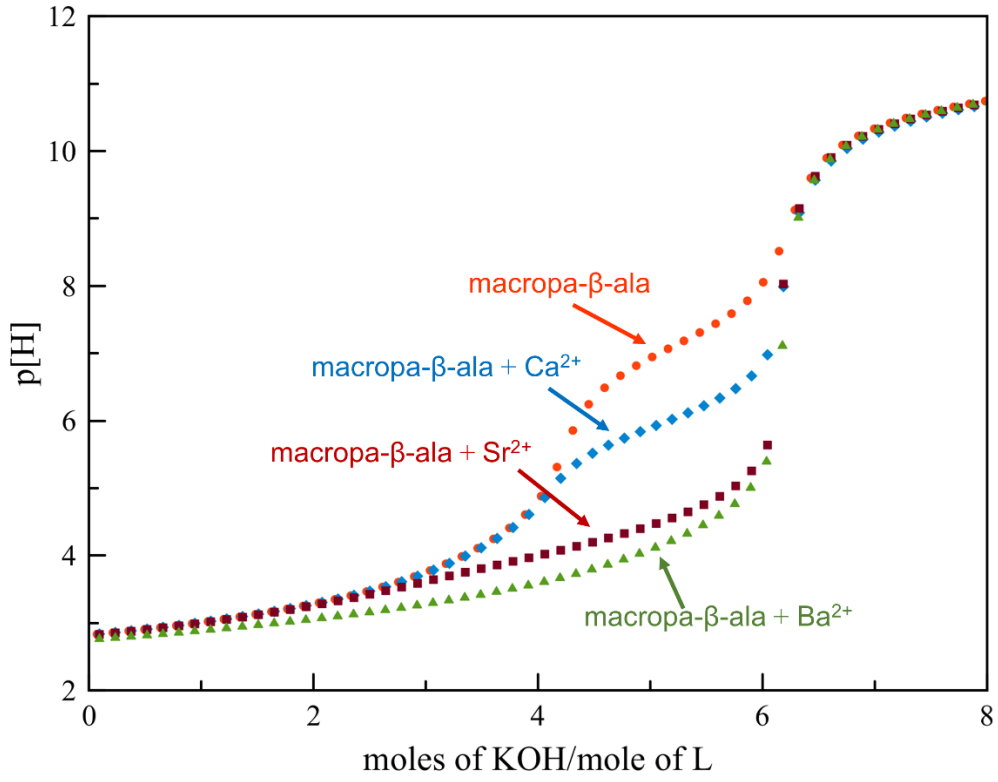

Fig. S15. Potentiometric titration curves for macropa-β-alanine in the presence and absence of 1 equiv of Ca^{2+}, Sr^{2+}, or Ba^{2+}. I = 0.1 M KCl, 25 °C

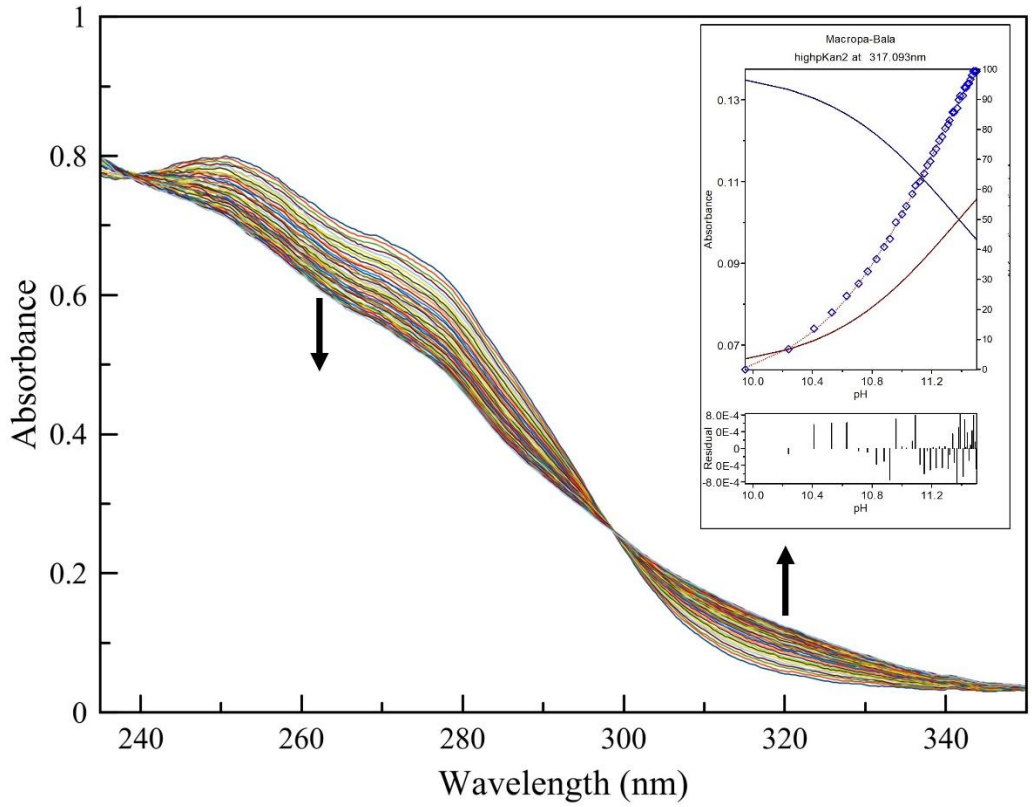

Fig. S16. Representative spectra of a simultaneous UV-potentiometric titration of a solution of macropa-β-alanine (0.210 mM) from pH 10 to 11.5. *I* = 0.1 M KCl, 25 °C, path length = 0.2 cm. Inset: Representative fit (dotted red line) of the data (blue diamonds) at λ = 317 nm using *HypSpec2014*.

2.8 Characterization of [Ba(macropa-β-alanine)] and [^{223}Ra][Ra(macropa-β-alanine)]

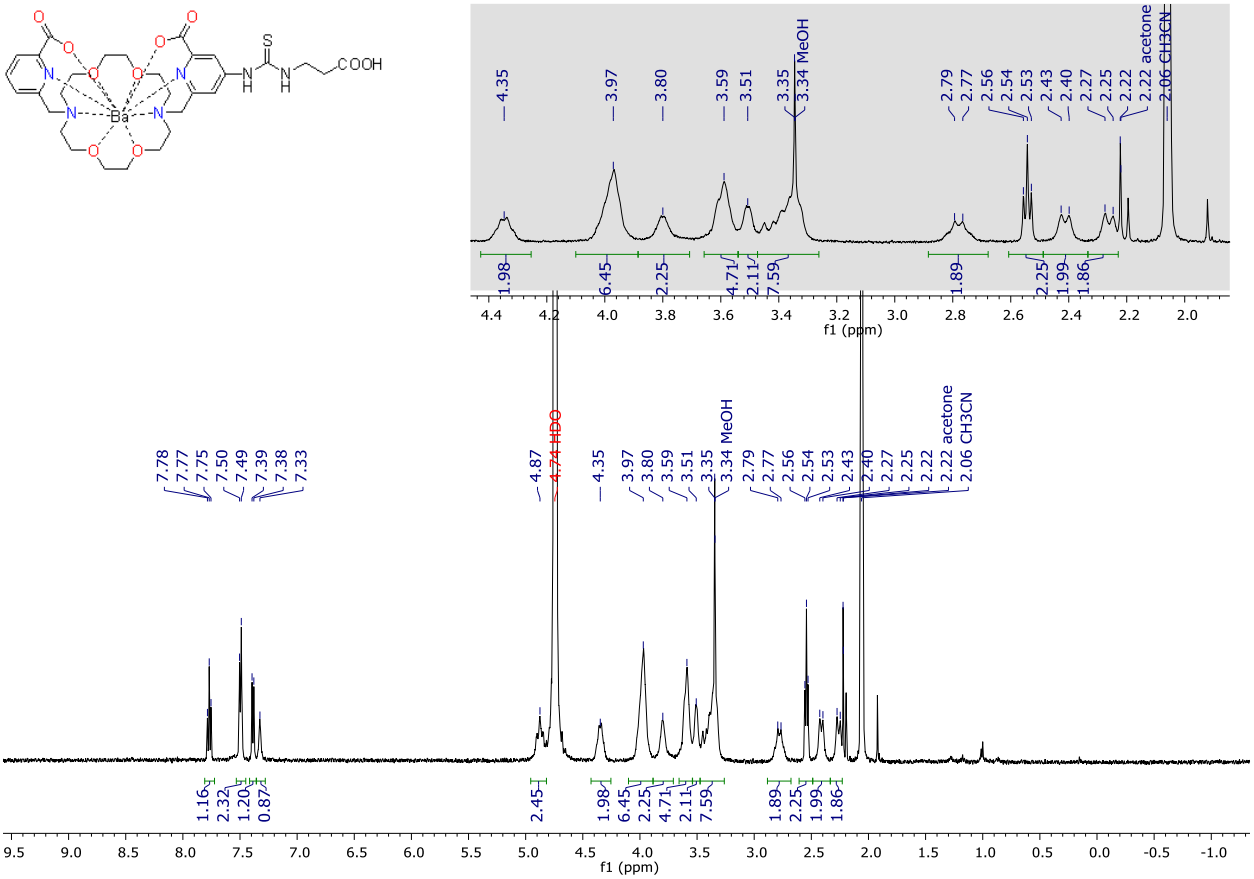

Fig. S17. ^{1}H NMR spectrum of [Ba(macropa-β-alanine)]. 500 MHz, D_2O. CH_3CN was added as an internal standard.

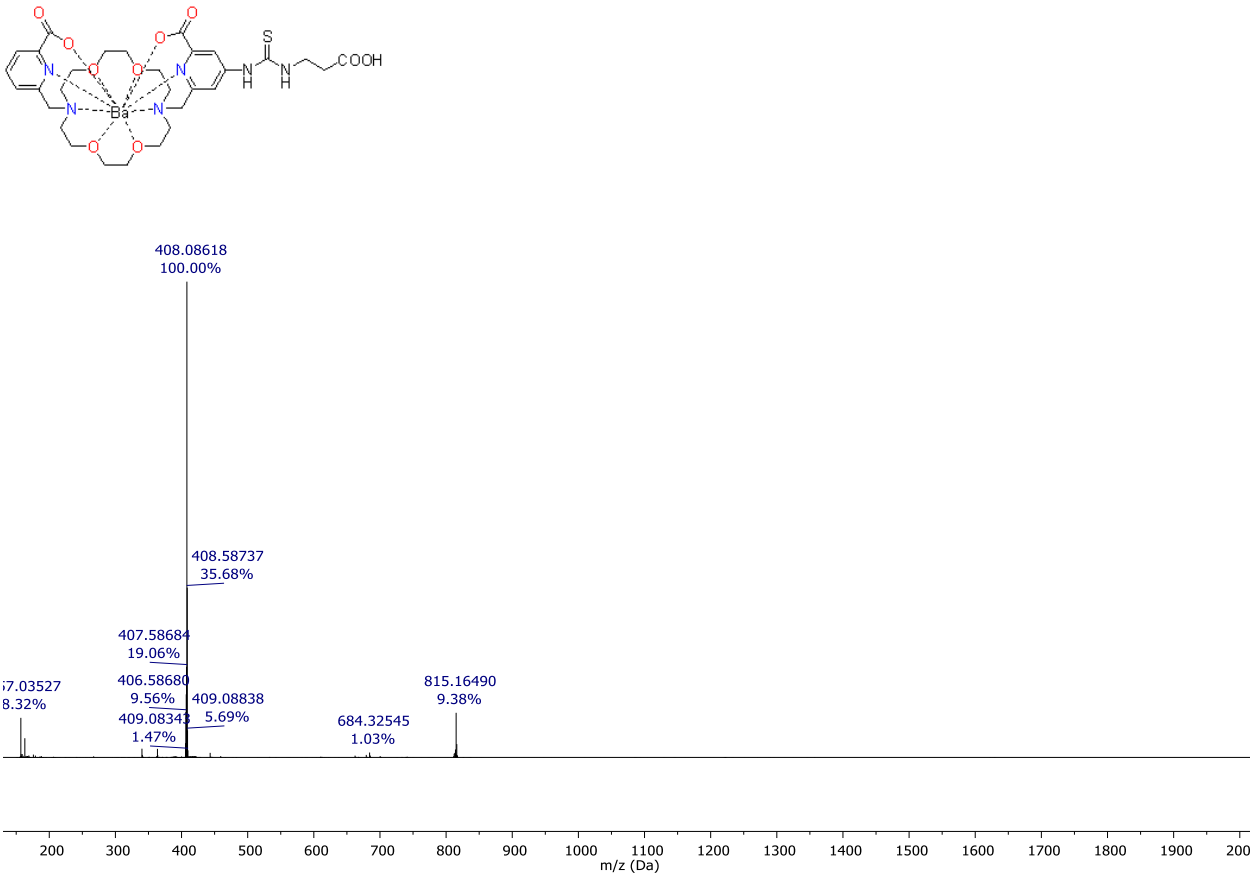

Fig. S18. ESI-HRMS of [Ba(macropa-β-alanine)]. The sample was diluted and analyzed using a mobile phase of CH_3CN:H_2O (1:1). Two ions were observed, corresponding to $[M+H]^+$ (*m/z* 815.16490) and $[M+2H]^{2+}$ (*m/z* 408.08618).

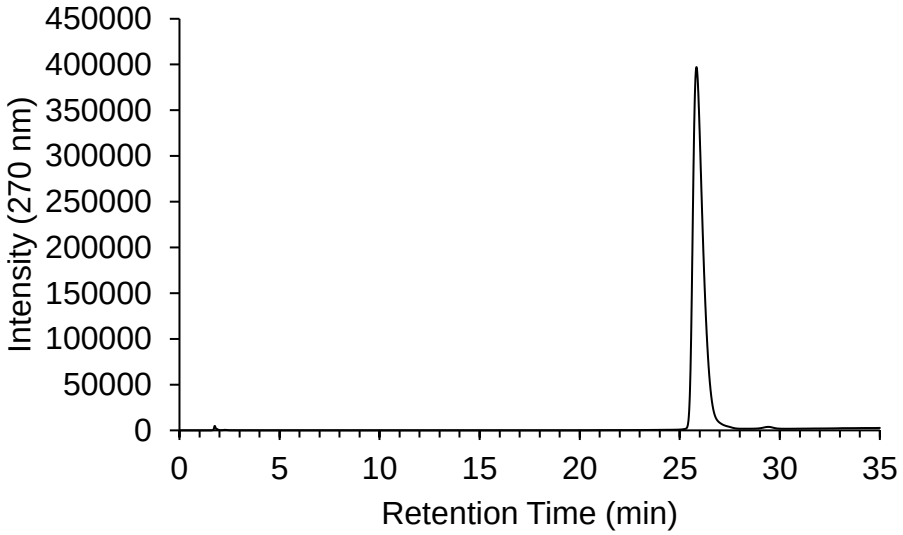

Fig. S19. HPLC chromatogram of [Ba(macropa-β-alanine)]. Retention time (t_R) = 25.84 min using a binary MeOH/H_2O mobile phase containing 10 mM NH_4HCO_3 (program: 0% MeOH for 10 min followed by a linear gradient to 100% MeOH over 35 min).

Table S5. Crystal data and structure refinement for [Ba(macropa-β-alanine)(DMSO)].

Compound	[Ba(macropa-β-alanine)(DMSO)]
Empirical Formula	$C_{32}H_{45}BaN_6O_{11}S_2$
Formula Weight	891.20
a (Å)	17.68270(10)
b (Å)	10.44220(10)
c (Å)	22.5408(2)
α(∘)	90
β (∘)	90
γ(∘)	90
V (Å^3)	4162.08(6)
Z	4
Crystal System	Orthorhombic
Space Group	*P*ca21
ρ_{calc} (Mg/m^3)	1.422
μ (mm^{-1})	8.864
T (K)	99.97(13) K
2θ range (^{o})	1.960 to 70.075
Independent Reflections	7895
R_{int}	0.0608
Number of Parameters	625
Largest diff. peak and hole	2.443/-0.580
GoF	1.123
R1/wR2 (all data)	0.0701/.2019
R1/wR2 (>2θ)	0.0697/0.2010

Table S6. Atomic coordinates ($\times 10^4$) and equivalent isotropic displacement parameters ($Å^2 \times 10^3$) for [Ba(macropa-β-alanine)DMSO]. U(eq) is defined as one third of the trace of the orthogonalized U^{ij} tensor.

	x	y	z	U(eq)
Ba	7595(1)	340(1)	5589(1)	44(1)
S(1A)	6345(3)	6249(5)	3347(2)	49(1)
S(1B)	4484(6)	3256(11)	3222(4)	103(3)
S(2)	7311(5)	-3597(6)	5655(7)	90(4)
S(7)	7828(8)	-3651(8)	5472(9)	124(7)
O(1)	8501(8)	2051(10)	4998(4)	70(3)
O(2)	9296(9)	3691(11)	4902(6)	99(5)
O(3)	6669(6)	2010(8)	6206(4)	54(2)
O(4)	5883(7)	3629(9)	6336(4)	74(3)
O(5)	9079(6)	-718(13)	5881(5)	78(3)
O(6)	8567(5)	-865(8)	4705(4)	58(2)
O(7)	6109(6)	-616(11)	5301(7)	90(4)
O(8)	6626(6)	-900(11)	6468(6)	83(3)
O(9)	7590(7)	-2324(11)	5587(17)	120(6)
O(10A)	3436(13)	7070(20)	3283(6)	84(6)
O(10B)	3898(15)	7839(19)	3199(9)	83(6)
O(11A)	3381(12)	6440(20)	2380(7)	77(5)
O(11B)	4349(13)	7480(20)	2349(10)	83(5)
N(2)	8114(11)	160(20)	6879(6)	94(5)
N(3)	7074(11)	241(14)	4325(6)	87(5)
N(4)	6770(20)	2460(40)	5025(11)	45(8)
N(5A)	5527(11)	5550(16)	4327(7)	42(3)
N(5B)	4796(17)	4380(20)	4279(11)	79(6)
N(6A)	4979(11)	7002(17)	3735(7)	55(3)
N(6B)	3926(14)	5190(18)	3727(8)	55(3)
N(29)	6600(20)	2270(40)	5027(12)	45(8)
C(1)	8901(8)	2901(12)	5212(7)	62(4)
C(3B)	9213(18)	4380(20)	6036(13)	71(6)
C(4B)	9230(20)	4440(30)	6650(13)	83(6)
C(5B)	8805(18)	3680(30)	7038(12)	81(6)
C(6A)	8619(10)	2101(16)	6792(4)	69(8)
N(1)	8525(6)	2252(11)	6184(4)	68(4)
C(2)	8953(9)	3153(12)	5878(5)	81(5)
C(3A)	9476(11)	3902(17)	6181(8)	84(8)
C(4A)	9570(12)	3750(20)	6789(8)	100(8)
C(5A)	9142(13)	2850(20)	7095(5)	87(7)
C(6B)	8419(19)	2590(20)	6811(13)	75(8)
C(7)	8041(13)	1500(30)	7126(6)	108(7)
C(8)	8940(15)	-330(30)	6917(9)	130(11)
C(9)	9073(11)	-1380(30)	6430(10)	118(9)
C(10)	9423(8)	-1451(19)	5449(10)	95(6)
C(11)	9323(9)	-837(15)	4833(8)	71(4)
C(12)	8425(14)	-380(13)	4129(7)	76(5)
C(13)	7565(15)	-680(30)	4030(11)	111(12)
C(14)	6352(17)	-290(30)	4259(13)	122(12)
C(15)	6108(13)	-1180(30)	4699(15)	129(12)
C(16)	5740(8)	-1412(17)	5710(14)	111(9)

C(17)	5838(10)	-810(20)	6302(15)	119(10)
C(18)	6804(14)	-490(20)	7054(11)	113(10)
C(19)	7617(14)	-610(50)	7258(14)	120(13)
C(20)	7144(14)	1560(20)	4078(6)	102(8)
C(21A)	6801(14)	2690(20)	4452(10)	42(4)
C(21B)	6530(17)	2240(30)	4447(11)	54(5)
C(22A)	6394(11)	3698(16)	4182(7)	40(3)
C(22B)	5934(18)	2910(30)	4165(10)	76(7)
C(23A)	5976(13)	4492(16)	4523(8)	41(4)
C(23B)	5439(15)	3640(20)	4479(9)	60(5)
C(24A)	5952(11)	4251(16)	5134(7)	35(3)
C(24B)	5558(19)	3670(30)	5088(10)	65(6)
C(25A)	6336(14)	3240(20)	5362(9)	40(5)
C(25B)	6107(16)	2950(30)	5352(9)	47(7)
C(26)	6276(8)	2913(10)	6034(5)	48(3)
C(27A)	5587(11)	6291(16)	3807(7)	38(3)
C(27B)	4250(20)	4100(30)	3816(11)	94(9)
C(28A)	4897(14)	7966(17)	3258(8)	50(4)
C(28B)	3295(18)	5270(40)	3289(12)	81(7)
C(29A)	4537(15)	7390(20)	2691(10)	59(5)
C(29B)	3580(20)	5840(30)	2695(12)	75(6)
C(30)	3823(9)	7037(15)	2773(5)	80(3)
C(31)	7480(20)	-4500(30)	6170(30)	190(30)
C(32)	7680(30)	-4330(40)	4930(30)	240(30)

Table S7. Bond lengths [Å] and angles [°] for [Ba(macropa-β-alanine)(DMSO)].

Ba-O(1)	2.745(10)
Ba-O(3)	2.767(9)
Ba-O(5)	2.923(10)
Ba-O(6)	2.916(9)
Ba-O(7)	2.885(11)
Ba-O(8)	2.923(10)
Ba-O(9)	2.782(12)
Ba-N(2)	3.055(13)
Ba-N(3)	2.995(13)
Ba-N(4)	2.94(4)
Ba-N(29)	2.96(4)
Ba-N(1)	2.914(9)
S(1A)-C(27A)	1.694(18)
S(1B)-C(27B)	1.65(2)
S(2)-O(9)	1.427(14)
S(2)-C(31)	1.52(6)
S(2)-C(32)	1.91(4)
S(7)-O(9)	1.471(14)
S(7)-C(31)	1.90(6)
S(7)-C(32)	1.43(5)
O(1)-C(1)	1.234(18)
O(2)-C(1)	1.287(16)
O(3)-C(26)	1.234(14)
O(4)-C(26)	1.228(15)
O(5)-C(9)	1.42(2)
O(5)-C(10)	1.38(2)
O(6)-C(11)	1.368(19)
O(6)-C(12)	1.42(2)
O(7)-C(15)	1.48(3)
O(7)-C(16)	1.40(3)
O(8)-C(17)	1.45(2)
O(8)-C(18)	1.42(3)
O(10A)-C(30)	1.337(17)
O(10B)-C(30)	1.280(18)
O(11A)-C(30)	1.336(17)
O(11B)-C(30)	1.411(19)
N(2)-C(7)	1.50(3)
N(2)-C(8)	1.55(3)
N(2)-C(19)	1.47(3)
N(3)-C(13)	1.46(2)
N(3)-C(14)	1.40(4)
N(3)-C(20)	1.49(3)
N(4)-C(21A)	1.31(2)
N(4)-C(25A)	1.35(2)
N(5A)-C(23A)	1.43(2)
N(5A)-C(27A)	1.41(2)
N(5B)-C(23B)	1.45(3)
N(5B)-C(27B)	1.46(3)
N(6A)-C(27A)	1.32(2)
N(6A)-C(28A)	1.48(2)
N(6B)-C(27B)	1.29(3)
N(6B)-C(28B)	1.49(3)
N(29)-C(21B)	1.31(2)

N(29)-C(25B)	1.34(2)
C(1)-C(2)	1.527(18)
C(3B)-C(4B)	1.39(3)
C(3B)-C(2)	1.41(2)
C(4B)-C(5B)	1.39(3)
C(5B)-C(6B)	1.42(2)
C(6A)-N(1)	1.3900
C(6A)-C(5A)	1.3900
C(6A)-C(7)	1.42(2)
N(1)-C(2)	1.3900
N(1)-C(6B)	1.47(3)
C(2)-C(3A)	1.3900
C(3A)-C(4A)	1.3900
C(4A)-C(5A)	1.3900
C(6B)-C(7)	1.50(3)
C(8)-C(9)	1.57(4)
C(10)-C(11)	1.54(3)
C(12)-C(13)	1.57(4)
C(14)-C(15)	1.42(4)
C(16)-C(17)	1.49(4)
C(18)-C(19)	1.51(3)
C(20)-C(21A)	1.57(3)
C(20)-C(21B)	1.54(3)
C(21A)-C(22A)	1.42(2)
C(21B)-C(22B)	1.41(3)
C(22A)-C(23A)	1.35(2)
C(22B)-C(23B)	1.36(3)
C(23A)-C(24A)	1.40(2)
C(23B)-C(24B)	1.39(3)
C(24A)-C(25A)	1.36(2)
C(24B)-C(25B)	1.37(3)
C(25A)-C(26)	1.56(2)
C(25B)-C(26)	1.57(2)
C(28A)-C(29A)	1.55(3)
C(28B)-C(29B)	1.55(3)
C(29A)-C(30)	1.33(3)
C(29B)-C(30)	1.33(3)

O(1)-Ba-O(3)	100.3(3)
O(1)-Ba-O(5)	80.3(4)
O(1)-Ba-O(6)	66.8(3)
O(1)-Ba-O(7)	130.4(4)
O(1)-Ba-O(8)	163.7(4)
O(1)-Ba-O(9)	130.7(5)
O(1)-Ba-N(2)	109.0(4)
O(1)-Ba-N(3)	75.0(5)
O(1)-Ba-N(4)	65.8(9)
O(1)-Ba-N(29)	72.4(9)
O(1)-Ba-N(1)	56.5(2)
O(3)-Ba-O(5)	131.0(3)
O(3)-Ba-O(6)	164.6(3)
O(3)-Ba-O(7)	78.0(3)
O(3)-Ba-O(8)	65.9(3)
O(3)-Ba-O(9)	129.0(5)
O(3)-Ba-N(2)	74.7(4)
O(3)-Ba-N(3)	108.6(3)

O(3)-Ba-N(4)	56.6(5)
O(3)-Ba-N(29)	55.5(5)
O(3)-Ba-N(1)	70.8(4)
O(5)-Ba-O(8)	101.9(3)
O(5)-Ba-N(2)	59.5(4)
O(5)-Ba-N(3)	118.5(4)
O(5)-Ba-N(4)	145.8(8)
O(5)-Ba-N(29)	152.7(9)
O(6)-Ba-O(5)	57.4(3)
O(6)-Ba-O(8)	128.1(3)
O(6)-Ba-N(2)	116.6(4)
O(6)-Ba-N(3)	61.1(4)
O(6)-Ba-N(4)	108.8(5)
O(6)-Ba-N(29)	110.6(5)
O(7)-Ba-O(5)	137.5(4)
O(7)-Ba-O(6)	103.5(3)
O(7)-Ba-O(8)	57.7(4)
O(7)-Ba-N(2)	117.9(5)
O(7)-Ba-N(3)	59.6(5)
O(7)-Ba-N(4)	73.2(9)
O(7)-Ba-N(29)	66.2(10)
O(7)-Ba-N(1)	148.7(3)
O(8)-Ba-N(2)	60.3(5)
O(8)-Ba-N(3)	116.7(5)
O(8)-Ba-N(4)	109.6(7)
O(8)-Ba-N(29)	104.0(8)
O(9)-Ba-O(5)	68.0(5)
O(9)-Ba-O(6)	64.5(6)
O(9)-Ba-O(7)	69.5(4)
O(9)-Ba-O(8)	63.7(6)
O(9)-Ba-N(2)	86.7(9)
O(9)-Ba-N(3)	87.8(8)
O(9)-Ba-N(4)	138.7(10)
O(9)-Ba-N(29)	132.6(10)
O(9)-Ba-N(1)	133.5(6)
N(3)-Ba-N(2)	174.6(5)
N(4)-Ba-N(2)	127.3(7)
N(4)-Ba-N(3)	57.5(6)
N(29)-Ba-N(2)	128.8(7)
N(29)-Ba-N(3)	55.5(6)
N(1)-Ba-O(5)	69.4(4)
N(1)-Ba-O(6)	106.1(3)
N(1)-Ba-O(8)	108.8(4)
N(1)-Ba-N(2)	55.5(4)
N(1)-Ba-N(3)	129.4(4)
N(1)-Ba-N(4)	87.9(8)
N(1)-Ba-N(29)	93.9(9)
O(9)-S(2)-C(31)	126(3)
O(9)-S(2)-C(32)	99(2)
C(31)-S(2)-C(32)	109(2)
O(9)-S(7)-C(31)	101.9(19)
C(32)-S(7)-O(9)	124(3)
C(32)-S(7)-C(31)	114(2)
C(1)-O(1)-Ba	127.9(9)
C(26)-O(3)-Ba	131.0(7)
C(9)-O(5)-Ba	112.0(10)

C(10)-O(5)-Ba	116.5(9)
C(10)-O(5)-C(9)	110.5(17)
C(11)-O(6)-Ba	115.0(9)
C(11)-O(6)-C(12)	111.0(14)
C(12)-O(6)-Ba	111.6(8)
C(15)-O(7)-Ba	110.1(12)
C(16)-O(7)-Ba	118.7(12)
C(16)-O(7)-C(15)	111.7(19)
C(17)-O(8)-Ba	111.1(11)
C(18)-O(8)-Ba	111.5(11)
C(18)-O(8)-C(17)	115.8(18)
S(2)-O(9)-Ba	158.9(8)
S(7)-O(9)-Ba	160.2(12)
C(7)-N(2)-Ba	105.7(10)
C(7)-N(2)-C(8)	112(2)
C(8)-N(2)-Ba	110.8(11)
C(19)-N(2)-Ba	114.0(16)
C(19)-N(2)-C(7)	104(2)
C(19)-N(2)-C(8)	110.3(18)
C(13)-N(3)-Ba	105.9(10)
C(13)-N(3)-C(20)	113(2)
C(14)-N(3)-Ba	113.3(17)
C(14)-N(3)-C(13)	103.5(18)
C(14)-N(3)-C(20)	113.5(19)
C(20)-N(3)-Ba	107.4(9)
C(21A)-N(4)-Ba	122.4(19)
C(21A)-N(4)-C(25A)	118(3)
C(25A)-N(4)-Ba	119.3(17)
C(27A)-N(5A)-C(23A)	129.7(17)
C(23B)-N(5B)-C(27B)	129(2)
C(27A)-N(6A)-C(28A)	123.5(19)
C(27B)-N(6B)-C(28B)	119(3)
C(21B)-N(29)-Ba	118(2)
C(21B)-N(29)-C(25B)	120(3)
C(25B)-N(29)-Ba	120.9(18)
O(1)-C(1)-O(2)	124.0(15)
O(1)-C(1)-C(2)	122.9(11)
O(2)-C(1)-C(2)	113.1(13)
C(4B)-C(3B)-C(2)	107(2)
C(3B)-C(4B)-C(5B)	126(3)
C(4B)-C(5B)-C(6B)	119(2)
N(1)-C(6A)-C(5A)	120.0
N(1)-C(6A)-C(7)	119.1(12)
C(5A)-C(6A)-C(7)	118.1(12)
C(6A)-N(1)-Ba	116.4(6)
C(2)-N(1)-Ba	122.9(6)
C(2)-N(1)-C(6A)	120.0
C(2)-N(1)-C(6B)	112.4(11)
C(6B)-N(1)-Ba	122.5(11)
C(3B)-C(2)-C(1)	115.1(15)
N(1)-C(2)-C(1)	109.8(9)
N(1)-C(2)-C(3B)	132.0(16)
N(1)-C(2)-C(3A)	120.0
C(3A)-C(2)-C(1)	128.2(10)
C(4A)-C(3A)-C(2)	120.0
C(3A)-C(4A)-C(5A)	120.0

C(4A)-C(5A)-C(6A)	120.0
C(5B)-C(6B)-N(1)	119(2)
C(5B)-C(6B)-C(7)	131(3)
N(1)-C(6B)-C(7)	109.0(16)
C(6A)-C(7)-N(2)	98.8(16)
C(6B)-C(7)-N(2)	119.5(18)
N(2)-C(8)-C(9)	109.6(19)
O(5)-C(9)-C(8)	106(2)
O(5)-C(10)-C(11)	110.8(14)
O(6)-C(11)-C(10)	107.1(12)
O(6)-C(12)-C(13)	103.3(18)
N(3)-C(13)-C(12)	112.2(19)
N(3)-C(14)-C(15)	117(2)
C(14)-C(15)-O(7)	112.5(19)
O(7)-C(16)-C(17)	106.6(13)
O(8)-C(17)-C(16)	109(2)
O(8)-C(18)-C(19)	118(2)
N(2)-C(19)-C(18)	110.4(19)
N(3)-C(20)-C(21A)	117.4(16)
N(3)-C(20)-C(21B)	99.8(19)
N(4)-C(21A)-C(20)	114(2)
N(4)-C(21A)-C(22A)	122(2)
C(22A)-C(21A)-C(20)	121.6(17)
N(29)-C(21B)-C(20)	119(2)
N(29)-C(21B)-C(22B)	121(3)
C(22B)-C(21B)-C(20)	121(2)
C(23A)-C(22A)-C(21A)	119.4(17)
C(23B)-C(22B)-C(21B)	121(2)
C(22A)-C(23A)-N(5A)	127.0(16)
C(22A)-C(23A)-C(24A)	117.8(17)
C(24A)-C(23A)-N(5A)	115.2(16)
C(22B)-C(23B)-N(5B)	130(2)
C(22B)-C(23B)-C(24B)	116(2)
C(24B)-C(23B)-N(5B)	114(2)
C(25A)-C(24A)-C(23A)	119.7(17)
C(25B)-C(24B)-C(23B)	122(2)
N(4)-C(25A)-C(24A)	123(2)
N(4)-C(25A)-C(26)	117.3(19)
C(24A)-C(25A)-C(26)	120.2(18)
N(29)-C(25B)-C(24B)	121(2)
N(29)-C(25B)-C(26)	114(2)
C(24B)-C(25B)-C(26)	125(2)
O(3)-C(26)-C(25A)	115.7(13)
O(3)-C(26)-C(25B)	115.8(13)
O(4)-C(26)-O(3)	127.6(11)
O(4)-C(26)-C(25A)	116.6(13)
O(4)-C(26)-C(25B)	114.9(14)
N(5A)-C(27A)-S(1A)	123.7(14)
N(6A)-C(27A)-S(1A)	125.9(14)
N(6A)-C(27A)-N(5A)	110.5(16)
N(5B)-C(27B)-S(1B)	121(2)
N(6B)-C(27B)-S(1B)	117.0(19)
N(6B)-C(27B)-N(5B)	103(2)
N(6A)-C(28A)-C(29A)	112.1(16)
N(6B)-C(28B)-C(29B)	110(2)
C(30)-C(29A)-C(28A)	113(2)

C(30)-C(29B)-C(28B)	111(2)
O(10B)-C(30)-O(11B)	103.1(18)
O(10B)-C(30)-C(29B)	138.3(19)
O(11A)-C(30)-O(10A)	106.4(16)
C(29A)-C(30)-O(10A)	126.8(16)
C(29A)-C(30)-O(11A)	126.3(16)
C(29B)-C(30)-O(11B)	115.2(18)

Table S8. Anisotropic displacement parameters ($Å^2 \times 10^3$) for [Ba(macropa-β-alanine)(DMSO)]. The anisotropic displacement factor exponent takes the form: $-2p^2[\, h^2 a^{*2} U^{11} + ... + 2\, h\, k\, a^*\, b^*\, U^{12}]$.

	U^{11}	U^{22}	U^{33}	U^{23}	U^{13}	U^{12}
Ba	39(1)	42(1)	51(1)	3(1)	-5(1)	-2(1)
S(1A)	63(3)	46(2)	39(2)	0(2)	9(2)	3(2)
S(1B)	93(6)	124(7)	94(6)	-55(5)	-14(5)	12(6)
S(2)	89(6)	40(3)	143(9)	-1(5)	45(6)	0(3)
S(7)	99(9)	47(4)	226(19)	9(7)	62(11)	12(4)
O(1)	92(8)	63(6)	55(5)	-7(4)	16(5)	-20(6)
O(2)	116(11)	57(5)	125(10)	-9(6)	59(9)	-33(6)
O(3)	68(6)	51(4)	42(4)	7(3)	4(4)	10(4)
O(4)	102(8)	69(5)	52(4)	0(4)	20(5)	18(6)
O(5)	44(5)	112(7)	77(6)	26(6)	-1(5)	12(6)
O(6)	51(5)	55(4)	70(5)	-8(4)	4(4)	-3(4)
O(7)	45(5)	74(5)	152(11)	-44(7)	-8(6)	-5(5)
O(8)	48(5)	78(6)	123(10)	40(6)	24(6)	3(5)
O(9)	99(8)	53(5)	209(17)	-25(14)	32(13)	-4(5)
O(10A)	102(14)	112(14)	37(7)	-5(8)	5(8)	-36(13)
O(10B)	94(15)	77(11)	77(10)	-8(8)	-2(11)	17(11)
O(11A)	89(13)	106(13)	35(7)	19(8)	-14(7)	-18(11)
O(11B)	90(14)	78(12)	82(13)	11(11)	-13(10)	-1(11)
N(2)	73(10)	162(14)	47(6)	34(8)	-6(7)	7(10)
N(3)	99(12)	96(10)	67(7)	-41(7)	-31(8)	50(9)
N(4)	55(17)	37(12)	42(7)	-8(7)	0(8)	-2(12)
N(5A)	51(9)	48(7)	27(6)	6(5)	5(6)	8(6)
N(5B)	115(16)	58(10)	63(11)	2(9)	-22(11)	20(11)
N(6A)	63(7)	61(7)	41(6)	3(5)	-5(5)	4(5)
N(6B)	63(7)	61(7)	41(6)	3(5)	-5(5)	4(5)
N(29)	53(16)	40(14)	42(8)	-7(8)	-6(8)	1(13)
C(1)	55(8)	43(6)	87(9)	-1(6)	26(7)	-14(5)
C(3B)	50(15)	62(14)	103(13)	-1(13)	-22(12)	8(12)
C(4B)	73(16)	67(13)	107(14)	-30(12)	-36(12)	12(11)
C(5B)	85(15)	99(15)	59(11)	-34(10)	-33(10)	18(12)
C(6A)	63(15)	103(19)	40(11)	-30(13)	3(10)	6(13)
N(1)	49(6)	97(9)	59(6)	-26(6)	-3(5)	-12(6)
C(2)	86(12)	71(9)	85(10)	-20(8)	20(9)	-28(9)
C(3A)	66(18)	60(16)	126(16)	-25(14)	-25(15)	-16(14)
C(4A)	83(17)	96(16)	122(15)	-34(14)	-31(14)	-15(13)
C(5A)	77(15)	93(16)	91(15)	-37(12)	-14(12)	5(12)
C(6B)	82(19)	87(16)	57(14)	-24(12)	-15(13)	18(13)
C(7)	108(14)	180(20)	37(6)	-8(9)	-3(8)	-17(16)
C(8)	68(13)	250(30)	69(10)	41(15)	-10(10)	31(15)
C(9)	55(10)	190(20)	112(16)	52(17)	-20(10)	15(14)
C(10)	39(6)	115(12)	131(18)	6(11)	17(8)	17(7)
C(11)	54(8)	68(8)	91(10)	0(7)	19(7)	-3(7)
C(12)	101(15)	68(9)	59(8)	-16(5)	22(9)	29(7)
C(13)	140(20)	140(17)	48(10)	-59(11)	-48(11)	84(17)
C(14)	91(18)	160(20)	118(18)	-87(18)	-65(16)	44(16)
C(15)	58(11)	140(20)	190(30)	-120(20)	-30(14)	14(12)
C(16)	42(6)	82(10)	210(30)	-31(15)	-3(12)	-13(7)

C(17)	39(8)	114(14)	200(30)	79(19)	22(12)	-13(9)
C(18)	78(14)	140(18)	120(18)	79(15)	52(13)	38(12)
C(19)	81(16)	210(30)	72(16)	70(19)	1(10)	27(16)
C(20)	148(18)	124(15)	34(5)	-10(7)	-7(8)	79(15)
C(21A)	47(11)	38(9)	42(7)	-6(7)	-5(8)	-8(7)
C(21B)	62(14)	56(13)	44(8)	-6(10)	-6(10)	7(11)
C(22A)	47(9)	39(7)	34(7)	-3(6)	-1(6)	-5(6)
C(22B)	89(15)	96(16)	44(9)	2(10)	-6(10)	28(13)
C(23A)	53(10)	31(7)	37(6)	-1(5)	-2(7)	-2(6)
C(23B)	86(12)	43(10)	51(8)	-1(8)	-2(8)	7(9)
C(24A)	42(9)	27(7)	34(6)	2(6)	0(6)	-1(7)
C(24B)	73(14)	70(14)	53(9)	-3(10)	-7(10)	16(12)
C(25A)	39(12)	38(10)	43(8)	4(7)	0(8)	0(9)
C(25B)	54(15)	45(13)	42(9)	17(8)	18(9)	0(11)
C(26)	61(7)	38(5)	45(5)	-10(4)	-6(5)	-3(5)
C(27A)	53(8)	32(7)	30(7)	-1(5)	-3(6)	-3(6)
C(27B)	150(20)	84(14)	51(11)	-7(10)	-31(13)	47(14)
C(28A)	65(12)	39(8)	45(9)	-4(6)	-13(8)	5(8)
C(28B)	55(13)	120(20)	71(13)	5(12)	-3(10)	10(12)
C(29A)	88(10)	53(11)	36(8)	14(8)	-27(8)	1(9)
C(29B)	81(16)	89(12)	56(11)	8(10)	-1(11)	12(11)
C(30)	92(8)	102(8)	46(5)	-4(5)	-18(5)	7(7)
C(31)	320(80)	54(15)	210(50)	-18(19)	100(40)	-12(15)
C(32)	350(70)	64(14)	320(60)	-70(30)	210(50)	-10(20)

Table S9. Hydrogen coordinates ($\times 10^4$) and isotropic displacement parameters ($Å^2 \times 10^3$) for [Ba(macropa-β-alanine)(DMSO)].

	x	y	z	U(eq)
H(5A)	5166	5766	4562	50
H(5B)	4730	5098	4460	94
H(6A)	4610	6900	3979	66
H(6B)	4073	5860	3916	66
H(3B)	9351	5034	5776	86
H(4B)	9547	5045	6820	99
H(5BA)	8777	3888	7439	97
H(3A)	9762	4505	5976	101
H(4A)	9920	4253	6991	121
H(5AA)	9205	2750	7502	104
H(7AA)	7547	1864	7046	129
H(7AB)	8142	1525	7548	129
H(7BC)	7505	1692	7150	129
H(7BD)	8232	1481	7529	129
H(8A)	9032	-695	7307	156
H(8B)	9290	372	6858	156
H(9A)	9551	-1813	6494	142
H(9B)	8670	-2010	6437	142
H(10A)	9203	-2302	5447	114
H(10B)	9957	-1534	5537	114
H(11A)	9505	39	4837	86
H(11B)	9605	-1313	4537	86
H(12A)	8736	-808	3835	91
H(12B)	8520	534	4111	91
H(13A)	7458	-680	3608	133
H(13B)	7456	-1534	4180	133
H(14A)	6333	-715	3877	146
H(14B)	5990	409	4246	146
H(15A)	6439	-1917	4693	155
H(15B)	5601	-1464	4603	155
H(16A)	5961	-2262	5707	133
H(16B)	5207	-1483	5613	133
H(17A)	5685	84	6286	142
H(17B)	5526	-1242	6593	142
H(18A)	6492	-977	7327	136
H(18B)	6657	399	7090	136
H(19A)	7658	-320	7666	144
H(19B)	7772	-1499	7242	144
H(20A)	6904	1565	3691	123
H(20B)	7677	1734	4017	123
H(20C)	7031	1580	3657	123
H(20D)	7642	1917	4147	123
H(22A)	6414	3814	3773	48
H(22B)	5880	2843	3755	92
H(24A)	5674	4783	5383	42
H(24B)	5257	4200	5321	79
H(28A)	5391	8312	3161	60
H(28B)	4584	8666	3400	60

H(28C)	2893	5797	3447	97
H(28D)	3092	4416	3219	97
H(29A)	4558	8021	2375	71
H(29B)	4830	6653	2567	71
H(29C)	3996	5322	2544	91
H(29D)	3180	5831	2405	91
H(31C)	7225	-5301	6104	289
H(31B)	8019	-4657	6183	289
H(31A)	7318	-4129	6532	289
H(31E)	7603	-3997	6508	289
H(31D)	6947	-4626	6142	289
H(31F)	7729	-5322	6197	289
H(32A)	7531	-5218	4913	364
H(32B)	7468	-3881	4601	364
H(32C)	8220	-4272	4922	364
H(32D)	7888	-5180	4960	364
H(32E)	7142	-4390	4873	364
H(32F)	7905	-3888	4606	364

Table S10. Torsion angles [°] for [Ba(macropa-β-ala)(DMSO)].

Ba-O(1)-C(1)-O(2)	-178.0(13)
Ba-O(1)-C(1)-C(2)	0(2)
Ba-O(3)-C(26)-O(4)	-179.0(10)
Ba-O(3)-C(26)-C(25A)	-4.0(18)
Ba-O(3)-C(26)-C(25B)	17(2)
Ba-O(5)-C(9)-C(8)	-67.4(18)
Ba-O(5)-C(10)-C(11)	42.0(16)
Ba-O(6)-C(11)-C(10)	55.4(14)
Ba-O(6)-C(12)-C(13)	-58.6(12)
Ba-O(7)-C(15)-C(14)	-57(2)
Ba-O(7)-C(16)-C(17)	45.2(16)
Ba-O(8)-C(17)-C(16)	58.2(18)
Ba-O(8)-C(18)-C(19)	-54(2)
Ba-N(2)-C(7)-C(6A)	-68.1(14)
Ba-N(2)-C(7)-C(6B)	-54(2)
Ba-N(2)-C(8)-C(9)	-37(2)
Ba-N(2)-C(19)-C(18)	-33(4)
Ba-N(3)-C(13)-C(12)	-52(3)
Ba-N(3)-C(14)-C(15)	-27(2)
Ba-N(3)-C(20)-C(21A)	-49(2)
Ba-N(3)-C(20)-C(21B)	-67.3(17)
Ba-N(4)-C(21A)-C(20)	14(4)
Ba-N(4)-C(21A)-C(22A)	179.1(18)
Ba-N(4)-C(25A)-C(24A)	178.6(19)
Ba-N(4)-C(25A)-C(26)	-2(4)
Ba-N(29)-C(21B)-C(20)	-20(4)
Ba-N(29)-C(21B)-C(22B)	164(3)
Ba-N(29)-C(25B)-C(24B)	-168(3)
Ba-N(29)-C(25B)-C(26)	16(4)
Ba-N(1)-C(2)-C(1)	-4.4(16)
Ba-N(1)-C(2)-C(3B)	154.1(18)
Ba-N(1)-C(2)-C(3A)	-169.7(10)
Ba-N(1)-C(6B)-C(5B)	-169(2)
Ba-N(1)-C(6B)-C(7)	24(3)
O(1)-C(1)-C(2)-C(3B)	-159.3(19)
O(1)-C(1)-C(2)-N(1)	3(2)
O(1)-C(1)-C(2)-C(3A)	166.9(15)
O(2)-C(1)-C(2)-C(3B)	19(2)
O(2)-C(1)-C(2)-N(1)	-178.9(13)
O(2)-C(1)-C(2)-C(3A)	-15(2)
O(5)-C(10)-C(11)-O(6)	-65.3(17)
O(6)-C(12)-C(13)-N(3)	80(2)
O(7)-C(16)-C(17)-O(8)	-68.8(18)
O(8)-C(18)-C(19)-N(2)	61(4)
N(2)-C(8)-C(9)-O(5)	71(2)
N(3)-C(14)-C(15)-O(7)	58(3)
N(3)-C(20)-C(21A)-N(4)	26(4)
N(3)-C(20)-C(21A)-C(22A)	-139(2)
N(3)-C(20)-C(21B)-N(29)	60(4)
N(3)-C(20)-C(21B)-C(22B)	-124(3)
N(4)-C(21A)-C(22A)-C(23A)	2(4)
N(4)-C(25A)-C(26)-O(3)	4(3)
N(4)-C(25A)-C(26)-O(4)	180(2)

N(5A)-C(23A)-C(24A)-C(25A)	177(2)
N(5B)-C(23B)-C(24B)-C(25B)	175(3)
N(6A)-C(28A)-C(29A)-C(30)	66(3)
N(6B)-C(28B)-C(29B)-C(30)	-63(3)
N(29)-C(21B)-C(22B)-C(23B)	3(6)
N(29)-C(25B)-C(26)-O(3)	-20(3)
N(29)-C(25B)-C(26)-O(4)	173(3)
C(1)-C(2)-C(3A)-C(4A)	-162.3(17)
C(3B)-C(4B)-C(5B)-C(6B)	12(5)
C(4B)-C(3B)-C(2)-C(1)	-180(2)
C(4B)-C(3B)-C(2)-N(1)	23(3)
C(4B)-C(5B)-C(6B)-N(1)	5(5)
C(4B)-C(5B)-C(6B)-C(7)	168(3)
C(5B)-C(6B)-C(7)-N(2)	-141(3)
C(6A)-N(1)-C(2)-C(1)	165.3(15)
C(6A)-N(1)-C(2)-C(3A)	0.0
N(1)-C(6A)-C(5A)-C(4A)	0.0
N(1)-C(6A)-C(7)-N(2)	68.0(19)
N(1)-C(2)-C(3A)-C(4A)	0.0
N(1)-C(6B)-C(7)-N(2)	24(3)
C(2)-C(3B)-C(4B)-C(5B)	-23(4)
C(2)-N(1)-C(6B)-C(5B)	-6(3)
C(2)-N(1)-C(6B)-C(7)	-172.7(19)
C(2)-C(3A)-C(4A)-C(5A)	0.0
C(3A)-C(4A)-C(5A)-C(6A)	0.0
C(5A)-C(6A)-N(1)-Ba	170.4(10)
C(5A)-C(6A)-N(1)-C(2)	0.0
C(5A)-C(6A)-C(7)-N(2)	-131.1(12)
C(6B)-N(1)-C(2)-C(1)	-168(2)
C(6B)-N(1)-C(2)-C(3B)	-9(3)
C(7)-N(2)-C(8)-C(9)	-155.0(17)
C(7)-N(2)-C(19)-C(18)	82(3)
C(7)-C(6A)-N(1)-Ba	-29.0(19)
C(7)-C(6A)-N(1)-C(2)	161(2)
C(7)-C(6A)-C(5A)-C(4A)	-161(2)
C(8)-N(2)-C(7)-C(6A)	52.6(17)
C(8)-N(2)-C(7)-C(6B)	67(2)
C(8)-N(2)-C(19)-C(18)	-158(3)
C(9)-O(5)-C(10)-C(11)	171.2(17)
C(10)-O(5)-C(9)-C(8)	161.0(16)
C(11)-O(6)-C(12)-C(13)	171.7(13)
C(12)-O(6)-C(11)-C(10)	-176.7(12)
C(13)-N(3)-C(14)-C(15)	87(2)
C(13)-N(3)-C(20)-C(21A)	-165.4(19)
C(13)-N(3)-C(20)-C(21B)	176.3(17)
C(14)-N(3)-C(13)-C(12)	-172(2)
C(14)-N(3)-C(20)-C(21A)	77(2)
C(14)-N(3)-C(20)-C(21B)	59(2)
C(15)-O(7)-C(16)-C(17)	175.0(17)
C(16)-O(7)-C(15)-C(14)	169.1(18)
C(17)-O(8)-C(18)-C(19)	178(2)
C(18)-O(8)-C(17)-C(16)	-173.4(16)
C(19)-N(2)-C(7)-C(6A)	171.6(16)
C(19)-N(2)-C(7)-C(6B)	-174(2)
C(19)-N(2)-C(8)-C(9)	90(3)
C(20)-N(3)-C(13)-C(12)	65(2)

C(20)-N(3)-C(14)-C(15)	-149.7(18)
C(20)-C(21A)-C(22A)-C(23A)	166(2)
C(20)-C(21B)-C(22B)-C(23B)	-173(3)
C(21A)-N(4)-C(25A)-C(24A)	-2(5)
C(21A)-N(4)-C(25A)-C(26)	177(3)
C(21A)-C(22A)-C(23A)-N(5A)	-179(2)
C(21A)-C(22A)-C(23A)-C(24A)	-2(3)
C(21B)-N(29)-C(25B)-C(24B)	-3(6)
C(21B)-N(29)-C(25B)-C(26)	-178(3)
C(21B)-C(22B)-C(23B)-N(5B)	-180(3)
C(21B)-C(22B)-C(23B)-C(24B)	0(5)
C(22A)-C(23A)-C(24A)-C(25A)	-1(3)
C(22B)-C(23B)-C(24B)-C(25B)	-4(5)
C(23A)-N(5A)-C(27A)-S(1A)	-13(3)
C(23A)-N(5A)-C(27A)-N(6A)	167(2)
C(23A)-C(24A)-C(25A)-N(4)	3(4)
C(23A)-C(24A)-C(25A)-C(26)	-176.5(19)
C(23B)-N(5B)-C(27B)-S(1B)	-32(5)
C(23B)-N(5B)-C(27B)-N(6B)	-165(3)
C(23B)-C(24B)-C(25B)-N(29)	6(5)
C(23B)-C(24B)-C(25B)-C(26)	-179(3)
C(24A)-C(25A)-C(26)-O(3)	-177.0(18)
C(24A)-C(25A)-C(26)-O(4)	-1(3)
C(24B)-C(25B)-C(26)-O(3)	164(3)
C(24B)-C(25B)-C(26)-O(4)	-2(4)
C(25A)-N(4)-C(21A)-C(20)	-165(3)
C(25A)-N(4)-C(21A)-C(22A)	0(5)
C(25B)-N(29)-C(21B)-C(20)	174(3)
C(25B)-N(29)-C(21B)-C(22B)	-2(6)
C(27A)-N(5A)-C(23A)-C(22A)	-24(4)
C(27A)-N(5A)-C(23A)-C(24A)	158(2)
C(27A)-N(6A)-C(28A)-C(29A)	91(3)
C(27B)-N(5B)-C(23B)-C(22B)	38(5)
C(27B)-N(5B)-C(23B)-C(24B)	-142(4)
C(27B)-N(6B)-C(28B)-C(29B)	-102(3)
C(28A)-N(6A)-C(27A)-S(1A)	-5(3)
C(28A)-N(6A)-C(27A)-N(5A)	174.7(17)
C(28A)-C(29A)-C(30)-O(10A)	-4(3)
C(28A)-C(29A)-C(30)-O(11A)	-175.4(18)
C(28B)-N(6B)-C(27B)-S(1B)	47(4)
C(28B)-N(6B)-C(27B)-N(5B)	-178(2)
C(28B)-C(29B)-C(30)-O(10B)	2(5)
C(28B)-C(29B)-C(30)-O(11B)	156(2)
C(31)-S(2)-O(9)-Ba	-103(7)
C(31)-S(7)-O(9)-Ba	146(7)
C(32)-S(2)-O(9)-Ba	134(7)
C(32)-S(7)-O(9)-Ba	-84(7)

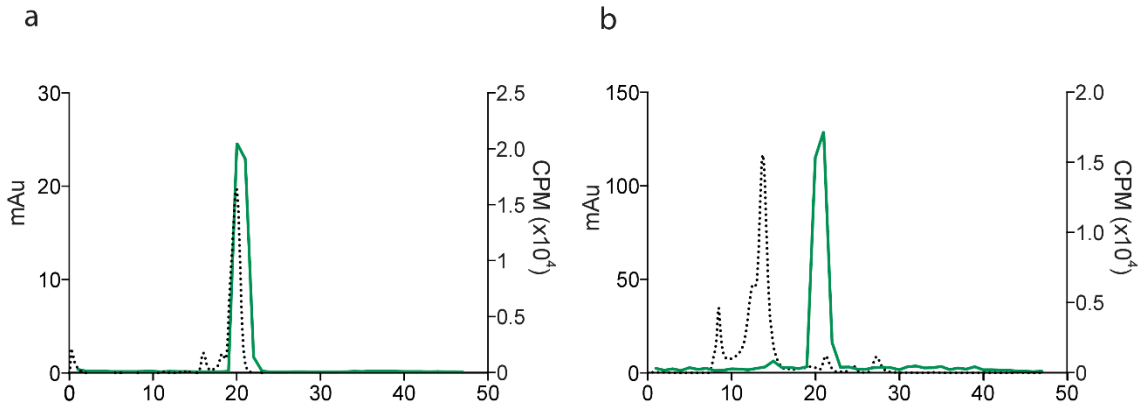

Fig. S20. Radiolabeling and stability of [^{223}Ra][Ra(macropa-β-alanine)]. a) SEC chromatogram of [^{223}Ra][Ra(macropa-β-alanine)] (black dashed line, absorbance at 280 nm; green solid line, gamma counting of fractions). b) SEC of [^{223}Ra][Ra(macropa-β-alanine)] challenged with serum for 12 days, showing intact [^{223}Ra][Ra(macropa-β-alanine)] (20 mL) and minor radioactivity associated with proteins (~5% at 10–15 mL).

2.9 Characterization of [Ba(macropa-DUPA)] and [^{223}Ra][Ra(macropa-DUPA)]

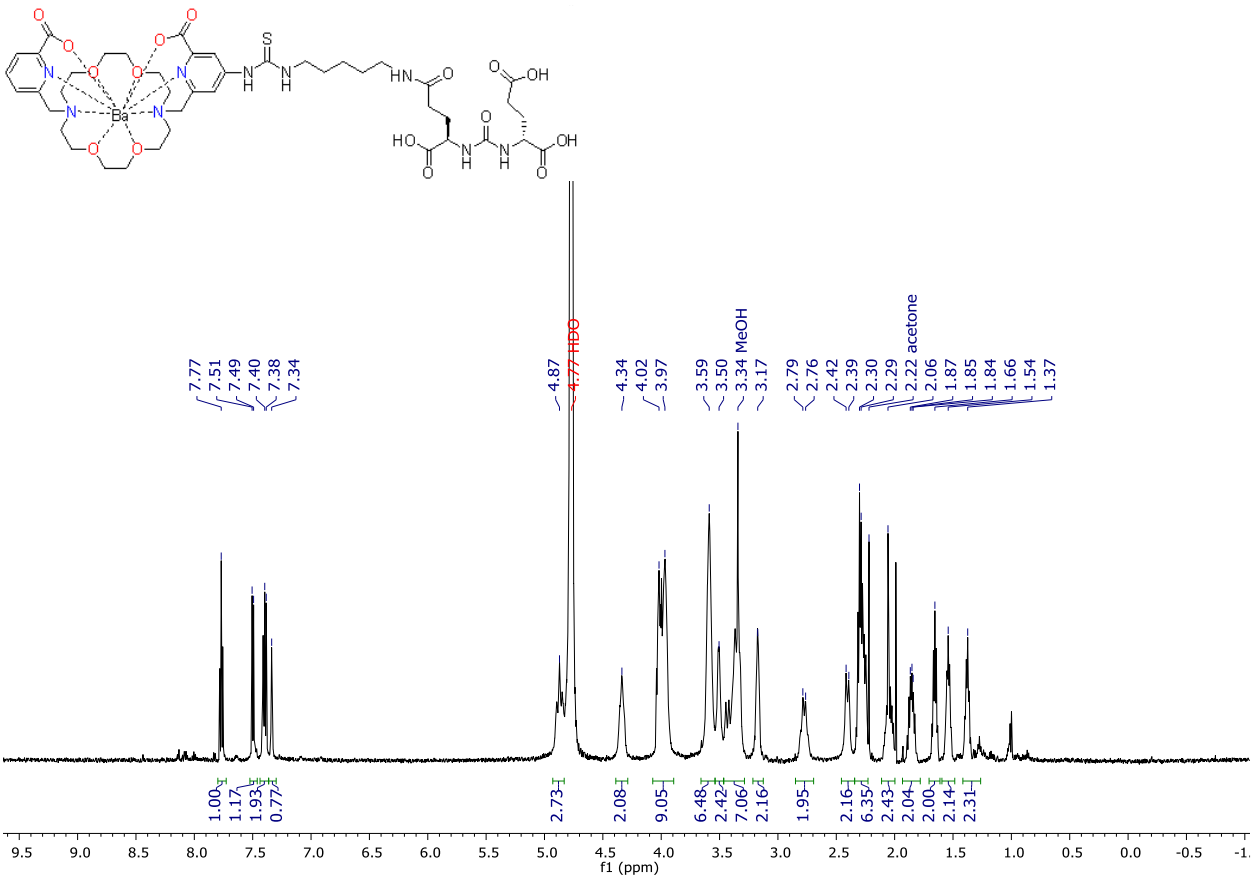

Fig. S21. ^{1}H NMR spectrum of [Ba(macropa-DUPA)]. 600 MHz, D_2O. The spectrum was referenced to an external standard of CH_3CN.

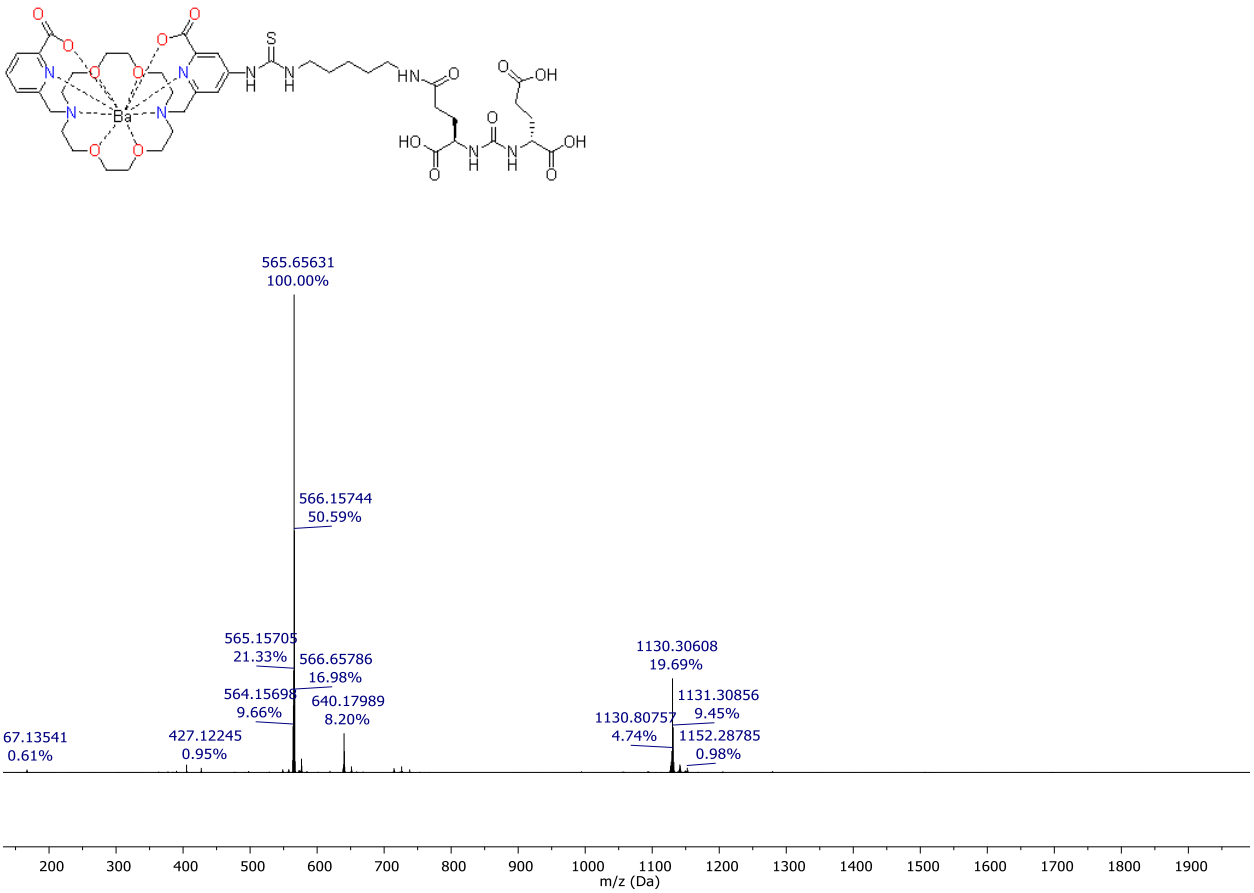

Fig. S22. ESI-HRMS of [Ba(macropa-DUPA)]. The sample was diluted in MeOH and analyzed using a mobile phase of CH_3CN:H_2O (1:1). Two ions were observed, corresponding to $[M+H]^+$ (*m/z* 1130.30608) and $[M+2H]^{2+}$ (*m/z* 565.65631).

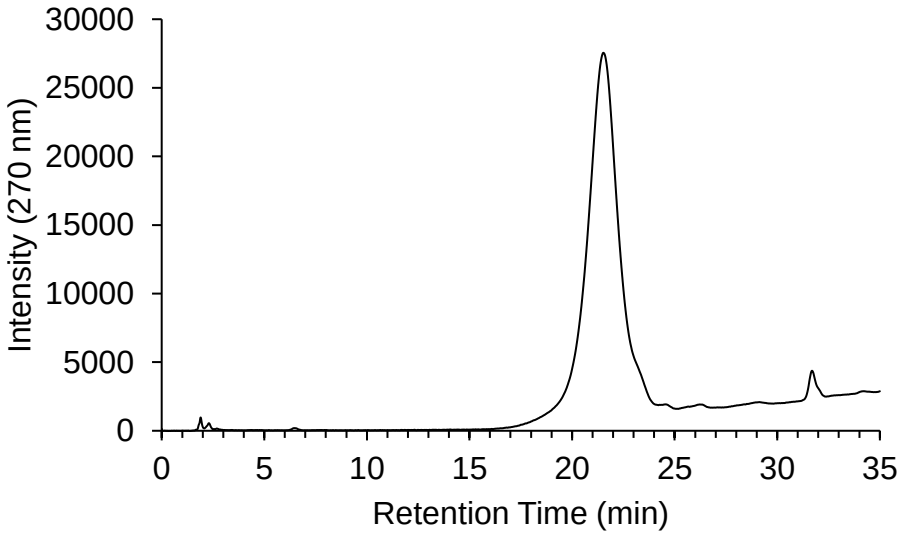

Fig. S23. HPLC chromatogram of [Ba(macropa-DUPA)]. Retention time (t_R) = 21.54 min using a binary MeOH/H_2O mobile phase containing 10 mM NH_4HCO_3 (program: 0% MeOH for 10 min followed by a linear gradient to 100% MeOH over 35 min).

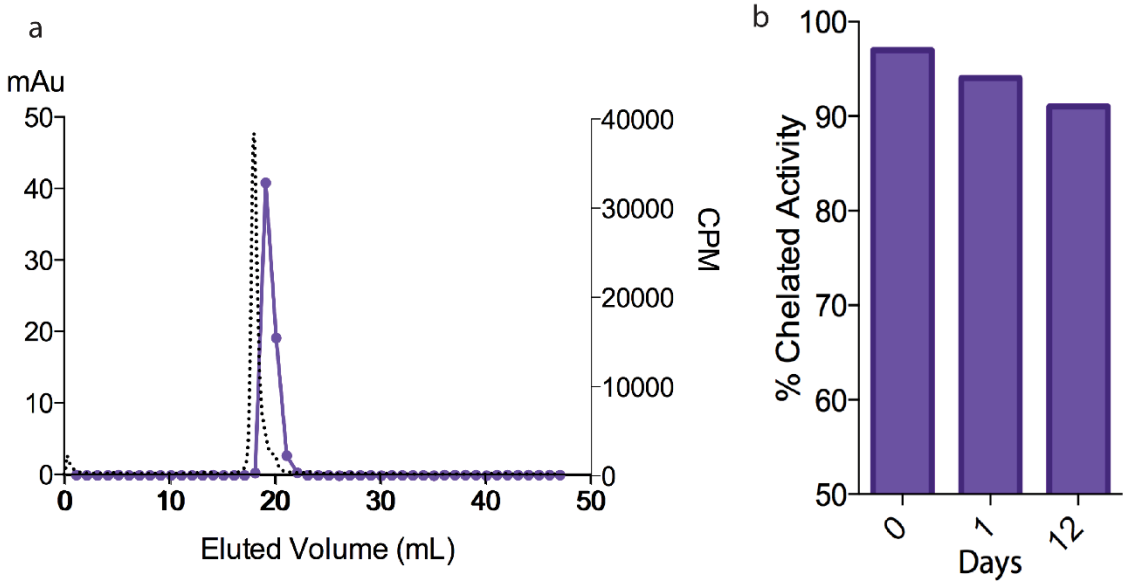

Fig. S24. Radiolabeling and stability of [^{223}Ra][Ra(macropa-DUPA)]. a) SEC of pure [^{223}Ra][Ra(macropa-DUPA] with a RL% exceeding 95% (n=5). b) Report of chelated activity following serum challenge over 12 days. Macropa chelation to ^{223}Ra when conjugated to a small-sized molecule appeared robust in an *ex vivo* setting with a radiometal retention exceeding 90% over 12 days.

2.10 In vivo radioactive organ distribution of [^{223}Ra][Ra(macropa-DUPA)]

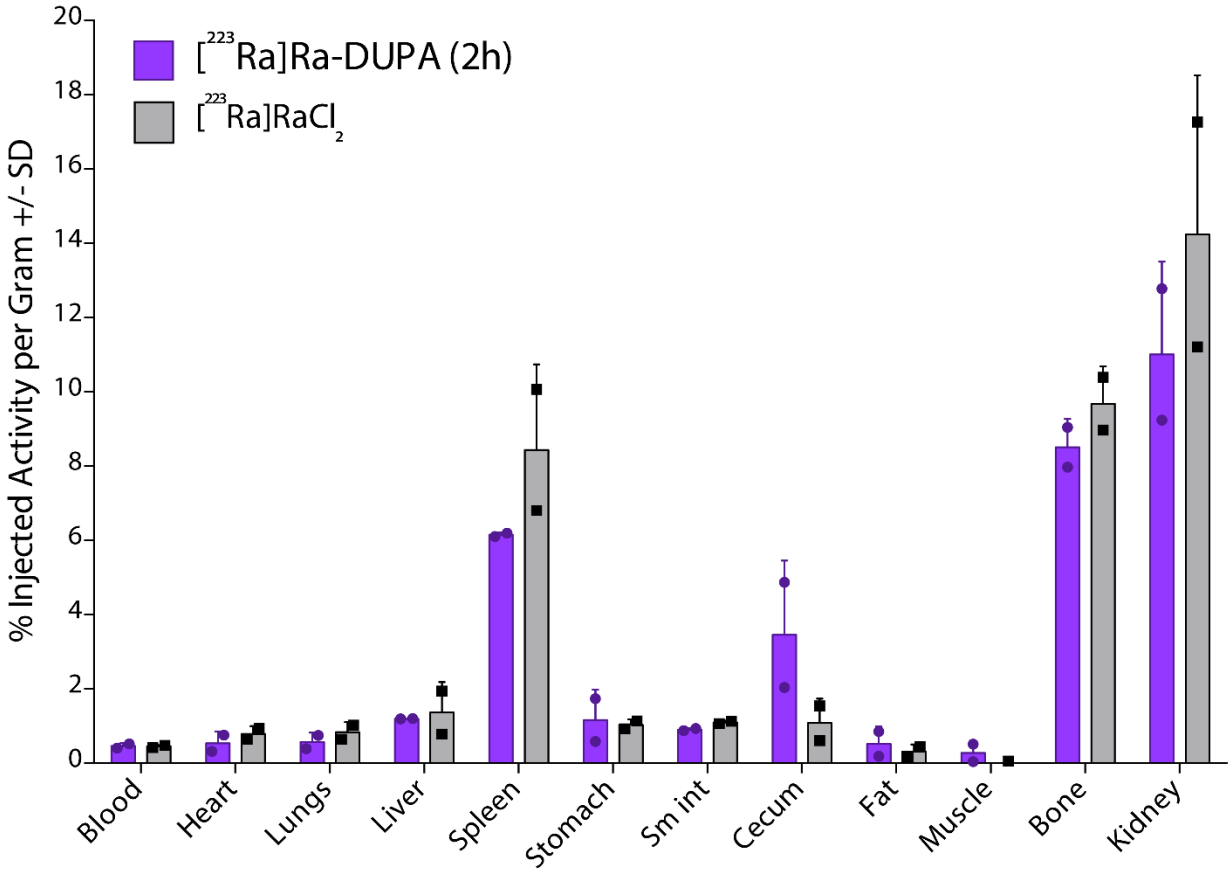

Fig. S25. *In vivo* evaluation of [^{223}Ra][Ra(macropa-DUPA)] 2h post-administration utilizing healthy, skeletally mature mice. The equal bone uptake observed when comparing [^{223}Ra][Ra(macropa-DUPA)] and [^{223}Ra]$RaCl_2$ highlights the instability of the radiocomplex in circulation.

2.11 Compilation of SE Chromatograms

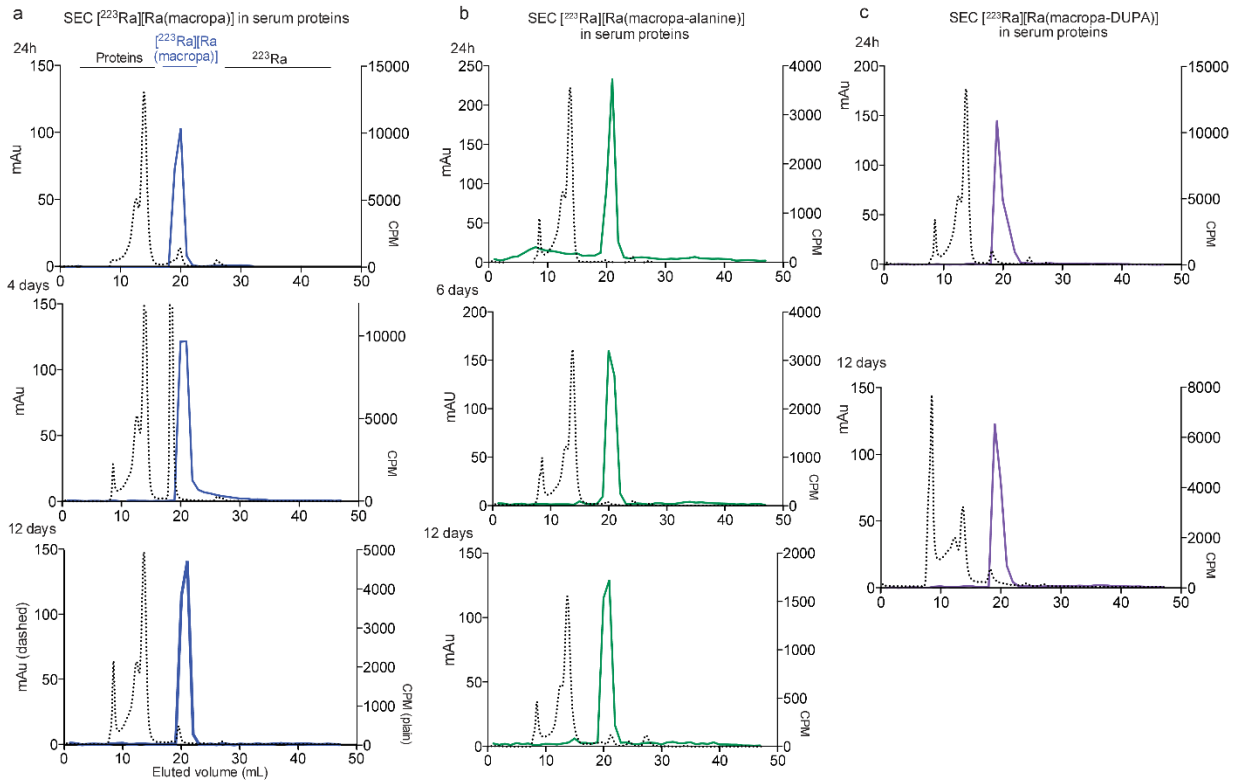

Fig. S26. Size exclusion chromatograms detected using UV (280 nm- dashed line plotted on left Y axes) and gamma counting (counts per minute – cpm plotted on right Y axes) of [^{223}Ra][Ra(macropa)] (left panel), [^{223}Ra][Ra(macropa-β-alanine)] (middle panel), and [^{223}Ra][Ra(macropa-DUPA)] (right panel) after 24 h, 6 d, and 12 d in human serum.

3. REFERENCES

1 M. J. Frisch, G. W. Trucks, H. B. Schlegel, G. E. Scuseria, M. A. Robb, J. R. Cheeseman, G. Scalmani, V. Barone, B. Mennucci, G. A. Petersson, H. Nakatsuji, M. Caricato, X. Li, H. P. Hratchian, A. F. Izmaylov, J. Bloino, G. Zheng, J. L. Sonnenberg, M. Hada, M. Ehara, K. Toyota, R. Fukuda, J. Hasegawa, M. Ishida, T. Nakajima, Y. Honda, O. Kitao, H. Nakai, T. Vreven, J. A. Montgomery, Jr., J. E. Peralta, F. Ogliaro, M. Bearpark, J. J. Heyd, E. Brothers, K. N. Kudin, V. N. Staroverov, R. Kobayashi, J. Normand, K. Raghavachari, A. Rendell, J. C. Burant, S. S. Iyengar, J. Tomasi, M. Cossi, N. Rega, N. J. Millam, M. Klene, J. E. Knox, J. B. Cross, V. Bakken, C. Adamo, J. Jaramillo, R. Gomperts, R. E. Stratmann, O. Yazyev, A. J. Austin, R. Cammi, C. Pomelli, J. W. Ochterski, R. L. Martin, K. Morokuma, V. G. Zakrzewski, G. A. Voth, P. Salvador, J. J. Dannenberg, S. Dapprich, A. D. Daniels, Ö. Farkas, J. B. Foresman, J. V. Ortiz, J. Cioslowski and D. J. Fox, *Gaussian09*, **2009**, Revision A.02; Gaussian Inc.: Wallingford, CT.

2 J. Tao, J. P. Perdew, V. N. Staroverov and G. E. Scuseria, *Phys. Rev. Lett.*, 2003, **91**, 146401.

3 V. N. Staroverov, G. E. Scuseria, J. Tao and J. P. Perdew, *J. Chem. Phys.*, 2003, **119**, 12129–12137.

4 A. Schäfer, H. Horn and R. Ahlrichs, *J. Chem. Phys.*, 1992, **97**, 2571–2577.

5 A. Schäfer, H. Horn and R. Ahlrichs, *J. Chem. Phys.*, 1994, **100**, 5829–5835.

6 I. S. Lim, H. Stoll and P. Schwerdtfeger, *J. Chem. Phys.*, 2006, **124**, 034107.

7 N. A. Thiele, S. N. MacMillan and J. J. Wilson, *J. Am. Chem. Soc.*, 2018, **140**, 17071–17078.

8 N. A. Thiele, V. Brown, J. M. Kelly, A. Amor-Coarasa, U. Jermilova, S. N. MacMillan, A. Nikolopoulou, S. Ponnala, C. F. Ramogida, A. K. H. Robertson, C. Rodríguez-Rodríguez, P. Schaffer, C. Williams Jr., J. W. Babich, V. Radchenko and J. J. Wilson, *Angew. Chem. Int. Ed.*, 2017, **56**, 14712–14717.

9 D. S. Abou, J. Pickett, J. E. Mattson and D. L. J. Thorek, *Appl. Radiat. Isot.*, 2017, **119**, 36–42.

10 M. Mato-Iglesias, A. Roca-Sabio, Z. Pálinkás, D. Esteban-Gómez, C. Platas-Iglesias, É. Tóth, A. de Blas and T. Rodríguez-Blas, *Inorg. Chem.*, 2008, **47**, 7840–7851.

11 A. Roca-Sabio, M. Mato-Iglesias, D. Esteban-Gómez, É. Toth, A. de Blas, C. Platas-Iglesias and T. Rodríguez-Blas, *J. Am. Chem. Soc.*, 2009, **131**, 3331–3341.

12 E. Aluicio-Sarduy, N. A. Thiele, K. E. Martin, B. A. Vaughn, J. Devaraj, A. P. Olson, T. E. Barnhart, J. J. Wilson, E. Boros and J. W. Engle, *Chem. Eur. J.*, 2020, **26**, 1238–1242.

13 N. A. Thiele, J. J. Woods and J. J. Wilson, *Inorg. Chem.*, 2019, **58**, 10483–10500.

14 P. Gans and B. O'Sullivan, *Talanta*, 2000, **51**, 33–37.

15 F. H. Sweeton, R. E. Mesmer and C. F. Baes, *J. Solution Chem.*, 1974, **3**, 191–214.

16 P. Gans, A. Sabatini and A. Vacca, *Talanta*, 1996, **43**, 1739–1753.

17 G. Jakab, C. Tancon, Z. Zhang, K. M. Lippert and P. R. Schreiner, *Org. Lett.*, 2012, **14**, 1724–1727.

18 G. Binzet, B. Zeybek, E. Klç, N. Külcü and H. Arslan, *J. Chem.*, 2013, 201238.

19 C. F. Baes and R. E. Mesmer, *The Hydrolysis of Cations*, Wiley, New York, 1976.

20 G. M. Sheldrick, *Acta Crystallogr. Sect. A*, 2015, **71**, 3–8.

21 G. M. Sheldrick, *Acta Crystallogr. Sect. A*, 2008, **64**, 112–122.

22 P. Müller, *Crystallogr. Rev.*, 2009, **15**, 57–83.

23 A. L. Spek, *Acta Crystallogr., Sect. D: Biol. Crystallogr.*, 2009, **65**, 148–155.